Journal of Volcanology and Geothermal Research 418 (2021) 107251

Contents lists available at ScienceDirect

Journal of Volcanology and Geothermal Research

journal homepage: www.elsevier.com/locate/jvolgeores

Morphometric classification and spatial distribution of Philippine volcanoes

Engielle Mae Paguican [a,b,*], Pablo Grosse [c,d], Gareth N. Fabbro [b,e], Matthieu Kervyn [a]

[a] Department of Geography, Earth System Sciences, Vrije Universiteit Brussel, Pleinlaan 2, Brussels 1050, Belgium
[b] College of Engineering and Geosciences, Caraga State University, Ampayon, Butuan City 8600, Philippines
[c] Consejo Nacional de Investigaciones Científicas y Técnicas (CONICET), Argentina
[d] Fundación Miguel Lillo, Miguel Lillo 251, San Miguel de Tucuman 4000, Argentina
[e] Earth Observatory of Singapore, Nanyang Technological University, 50 Nanyang Avenue, 639798, Singapore

ARTICLE INFO

Article history:
Received 13 September 2020
Received in revised form 9 April 2021
Accepted 12 April 2021
Available online 19 April 2021

Keywords:
Philippine volcanoes
Volcano morphometry
Principal component analysis
Cluster analysis
Volcano growth
Volcano spatial distribution

ABSTRACT

The Philippine Island Arc has a large number of volcanoes with diverse morphologies, making it an ideal location to study the factors controlling the morphology and spatial distribution of island arc volcanoes. We have identified 731 volcanic edifices using the SRTM 30 m digital elevation model, and computed their quantitative morphology using the MORVOLC algorithm. Hierarchical classification by principal component (PC) analysis distinguishes four volcano types: small flat cones, small steep cones, large cones, and massifs, with mean volumes of 0.2 km^3 (<6.2 km^3), 0.4 km^3 (<9 km^3), 29 km^3 (0.15–178 km^3), 267 km^3 (76–675 km^3), mean heights of 125 m (16–721 m), 260 m (53–971 m), 842 m (59–2313 m), 1533 m (1012–2175 m), and mean slopes of 13° (3–21°), 22° (14–37°), 15° (3–28°), 15° (11–22°), respectively. This classification is based mainly on their size and irregularity (PC1) and steepness (mean slope and height/basal width ratio; PC2), and to a lesser extent on the size of the summit region and edifice truncation (PC3) and edifice elongation (PC4). These morphological volcano classes represent stages along an evolutionary trend. The small flat cones are mostly monogenetic, whereas the small steep cone class represents an early growth stage. Some can develop into large polygenetic cones while a few can further grow laterally into massifs, both of which are preferentially found on thickened crust. There is a trend towards more silicic compositions from small to large cones, perhaps due to larger edifice loads preventing mafic dykes from reaching the surface. The distribution and alignment of the edifices within volcanic fields seems to be influenced by both regional and local stress fields and pre-existing structures.

© 2021 The Authors. Published by Elsevier B.V. This is an open access article under the CC BY license (http://creativecommons.org/licenses/by/4.0/).

1. Introduction

The evolution of the shape and size of a volcanic edifice depends on the prevailing constructive (i.e., eruption, intrusion, and deposition) and destructive (i.e., deformation and erosion) processes (e.g., McGuire, 1996; Tibaldi et al., 2008; Grosse et al., 2012; Thouret et al., 2014; Paguican and Bursik, 2016). Volcano morphology is a reflection of factors including age, growth stage, composition, vent position and migration, eruption rate, degree of erosion, deformation, and ultimately underlying constraints including magma flux and tectonic setting (Grosse et al., 2009). Thus, the quantification of volcano morphology (i.e., morphometry) and the resulting classifications can provide clues to the processes that interact during the growth of volcanoes and the factors that control them.

The Philippine archipelago is in an ideal tectonic setting for volcanism and earthquakes (Philippine Institute of Volcanology and Seismology, 2008), and contains one of the greatest concentrations of volcanoes on Earth. We have compiled a new database comprising over 700 volcanic edifices. Analysing the morphometry of the identified volcanoes at different inferred stages of growth, we suggest a growth pattern and evolutionary trend. We compare the morphology of the edifices with their geochemical composition and spatial distribution to investigate the influence of the regional stress field and active tectonic faults. Understanding the morphological changes associated with the stages of volcano growth can help in the initial assessment of volcanic hazards, which is useful in volcanic regions with limited resources.

2. The Philippine island arc

2.1. Geological setting

The Philippine archipelago (Fig. 1) is a composite terrane with continental, oceanic, island arc, and ophiolitic affinities (e.g., Barrier et al., 1991;

* Corresponding author at: College of Engineering and Geosciences, Caraga State University, Ampayon, Butuan City 8600, Philippines.
E-mail address: engiellepaguican@gmail.com (E.M. Paguican).

https://doi.org/10.1016/j.jvolgeores.2021.107251
0377-0273/© 2021 The Authors. Published by Elsevier B.V. This is an open access article under the CC BY license (http://creativecommons.org/licenses/by/4.0/).

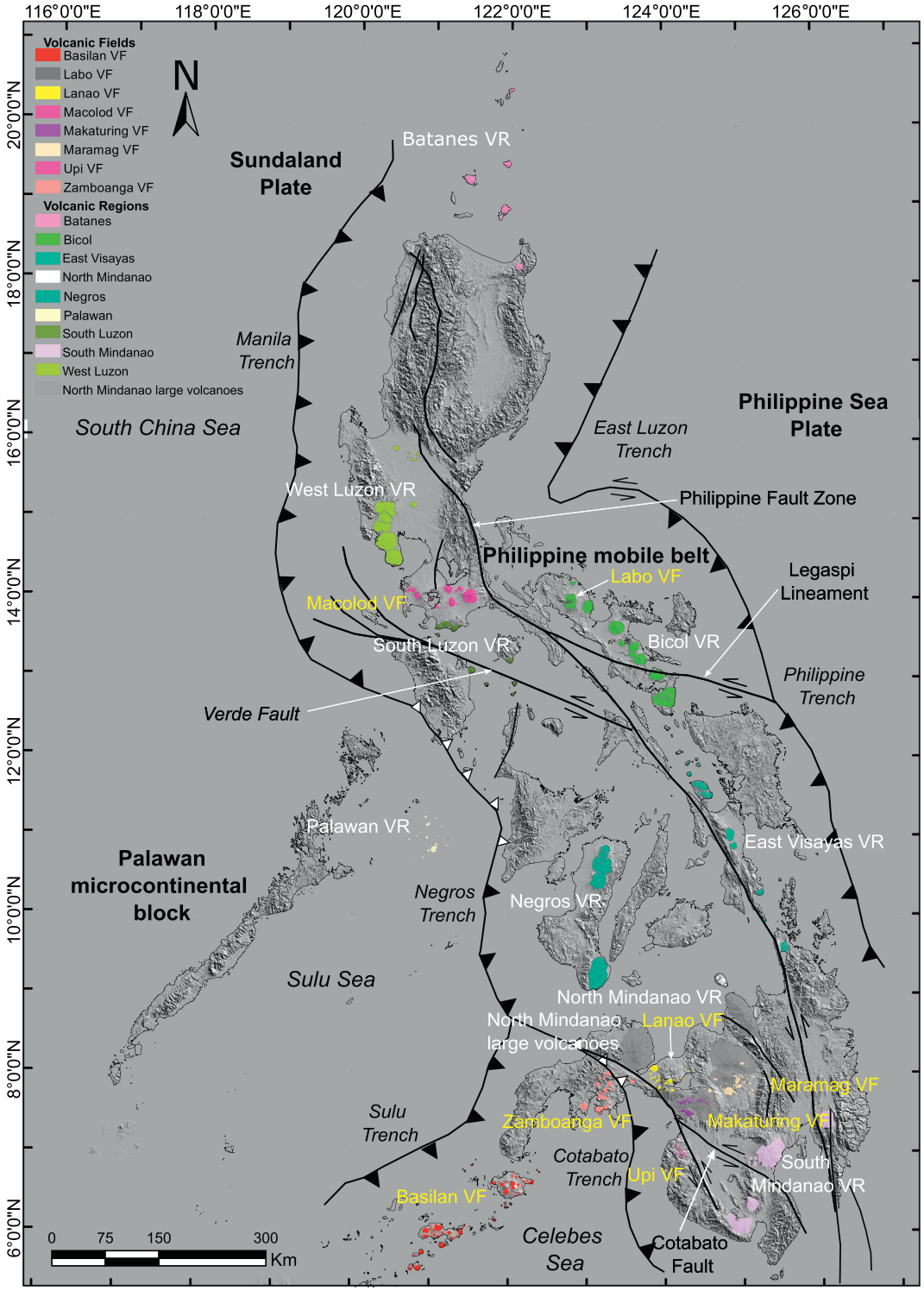

Fig. 1. Structural map of the Philippines with locations of the 731 analysed volcanic edifices. Lines with black triangles are active subduction zones, whereas those with white triangles are active collision fronts. Also shown are the major strike-slip faults that accommodate stress not accommodated by the subduction zones: the Philippine Fault Zone, Verde Fault, Legazpi Lineament, and Cotabato Fault.

Aurelio, 2000), and comprises two distinct geologic entities: the Palawan microcontinental block and the Philippine mobile belt (e.g., Gervasio, 1967; Yumul et al., 2005). Stress–strain relationships caused by the interaction of three major plates—the Sundaland, Philippine Sea and, to a certain extent, Indo-Australian plates—manifest in both the regional and local setting of the archipelago. The surrounding subduction systems accommodate most of the stresses generated within the island arc system. Excess stress caused by the oblique convergence is taken up by the left-lateral Philippine Fault Zone and regional faults including the Legazpi Lineament in southeast Luzon, which acts as a transfer fault connecting the Philippine Fault with the Philippine Trench (Fig. 1; Armada et al., 2012; Hsu et al., 2016).

Opposing subduction zones control Philippine tectonics: the Manila, Negros, Sulu, and Cotabato trenches on the west have eastward vergence, whereas the Philippine Sea Plate on the east subducts westward underneath the Philippine archipelago along the Philippine and East Luzon trenches (Fig. 1; Barrier et al., 1991; Aurelio, 2000). This unique tectonic setting makes the Philippines ideal for volcano formation. Moreover, this tectonic setting may control volcano edifice growth, as seen, for example, at Iriga (Paguican et al., 2012) and at other volcanoes in southern Luzon (Lagmay et al., 2000; Pasquarè and Tibaldi, 2003).

2.2. Philippine volcanoes

A list of 24 active and several potentially active volcanoes in the Philippines is available from the Philippine Institute of Volcanology and Seismology (2008). In the literature, Philippine volcanoes are divided into five volcanic arcs along the major subduction zones bounding the archipelago (Fig. 1; e.g., Aurelio and Pena, 2002). Volcanoes in the Luzon, Negros, Sulu–Zamboanga, West Mindanao, and Central Mindanao volcanic arcs are related to the subduction of Sundaland marginal basins (e.g., the South China, Sulu, and Celebes seas) along the Manila, Negros, Sulu, and Cotabato trenches, respectively. This subduction began during the Oligocene and continued until the early Miocene. When Palawan collided with Mindoro at ~9 to 8 Ma, it locked the convergence on the western side of the Philippines and subduction flipped to the east. Here, the Philippine Sea Plate has been subducted underneath the Philippine archipelago along the Philippine Trench since 5 Ma (Barrier et al., 1991).

From north to south, Batanes (also called Babuyan), West Luzon (referred to as the Bataan arc front to the west and Bataan back arc to the east), Macolod Corridor, and South Luzon (also called Mindoro by Castillo and Newhall, 2004) comprise the Luzon Volcanic Arc. The West Luzon and South Luzon segments have K-Ar dates of 1.7–0.1 Ma (Defant et al., 1990; Yumul et al., 2000b). The Macolod Corridor segment is a 40 km wide, northeast–southwest-trending area containing ~200 monogenetic volcanoes generated by counter-clockwise block rotation in southwestern Luzon (Calibo et al., 2009). The rotation is linked to the opposing motion of the subducting South China Sea under the Manila Trench on the west and the strike-slip Philippine Fault on the east coupled with shearing from the Verde Fault (Fig. 1). This block rotation resulted in localized extension along the sides of the blocks that led to partial melting of the crust (Galgana et al., 2007).

The East Philippine Volcanic Arc runs from Bicol to eastern Mindanao, which we segment into the Labo Volcanic Field and the Bicol and East Visayas volcanic regions (e.g., Andal et al., 2005). The Negros Volcanic Arc consists of four volcanoes on the island of Negros. The Sulu–Zamboanga Volcanic Arc is defined by fields of small monogenetic volcanoes along the boundary between the Sulu and Celebes seas, and is thought to be in its solfataric stage (Sajona et al., 1996). The Pliocene–Quaternary Zamboanga Volcanic Field is located in the southeastern portion of the Zamboanga Peninsula, and continues to the southwest as a set of small volcanic islands in Basilan, with its northern boundary near the trench axis. It is separated from the West and Central Mindanao volcanic fields by the Cotabato Fault. The West Mindanao Volcanic Arc is composed of stratovolcanoes and the volcanic fields of Makaturing, Lanao, and Upi (Pubellier et al., 1991). The Central Mindanao Volcanic Arc includes the stratovolcanoes of the North and South Mindanao volcanic regions and the Maramag Volcanic Field. It forms the most extensive region of active volcanoes in the Philippines (Sajona et al., 1993). The regional tectonic setting and seismic data suggest that the Neogene–Quaternary volcanic centres along this arc occur ~150–200 km above a westward-dipping Wadati–Benioff zone, and may be due to subduction along the Philippine trench (Corpuz, 1992); however, several later seismic (e.g., Besana et al., 1997; Pubellier et al., 1991) and petrological (e.g., Sajona et al., 1994) studies have suggested that volcanism in this area is associated with remnants of the Molucca Sea plate subducted under Mindanao.

3. Methodology

3.1. Database of Philippine volcanoes

We used the 30-m resolution Shuttle Radar Topography Mission (SRTM) digital elevation model (DEM) as an input for generating topographical data including slope, slope orientation, and shaded relief maps with varying sun azimuths and elevation angles in RSI ENVI. Additional open source data such as river and road systems were also used to identify volcanoes (http://philgis.org/). Rivers are useful because on conical morphological features such as volcanoes, they are usually organized in a radial pattern, and road networks are often constructed along volcano bases. We systematically mapped local lineaments and major faults described by Barrier et al. (1991) and Aurelio (2000) on volcano edifices or within the vicinity of volcanic fields. Conical topographic features (an identifiable broad base that tapers into a peak or more complex top) were then interpreted to be volcanoes. Their bases were drawn along breaks in slope, guided by river systems and road networks. Bases outlines were then imported into Google Earth to cross-check with satellite images that the features are indeed volcanoes. To minimise the number of edifices mis-identified as volcanoes, we also compared our results with previous publications (e.g., Knittel and Oles, 1994; Sajona et al., 1997; Vogel et al., 2006), and geological, topographical, and geohazard maps from the Mines and Geosciences Bureau, including the geologic map of the Philippines from Aurelio and Pena (2002). The edifice base outlines do not include long-runout lahar, pyroclastic flow, and debris avalanche deposits. In addition, some volcanoes may continue underwater and their real edifice bases may be on the seafloor. The following criteria was used for defining volcano bases.

1. They have a closed circular or elliptical outline with positive relief for stratovolcanoes and cones, whereas maars and calderas show mostly negative relief (Fig. 2A).
2. They are characterized by a break in slope, concave for cones and convex for maars and calderas.
3. Volcanic edifices were interpreted based only on morphology. For parasitic cones or overlapping edifices, each individual edifice was drawn separately, but the spatial relationships with the neighbouring volcanoes were noted for consideration of the buttressing and gravity effects on the morphological classification (Fig. 2A).
4. For edifices that regrew after collapse or erosion (Fig. 2B), we separately delineated the base of the younger and older edifices.

We also manually delineated summit craters formed by eruptions and summit openings such as collapse scars and erosional amphitheatres. Collapse scars (referred to as volcanic landslide scars by Bernard et al., 2020) are horseshoe-shaped and formed by rapid large-scale collapse events, including debris avalanches and large landslides. Erosional breaches are similar to scars, and are formed by long-lived, small-scale fluvial processes (Karátson et al., 1999). These features can overlap (e.g., breached summit craters).

3.2. Edifice morphometry

The volcano base outlines and the 30-m resolution DEM were the input data for MORVOLC, an interactive data language (IDL)-based code that generates morphometric parameters that describe the size (height, width, and volume), plan shape (ellipticity and irregularity indexes), and profile shape (height/basal width ratio, summit width/basal width ratio, and slope) of each volcanic edifice (Grosse et al., 2012). MORVOLC uses the volcano base outline to compute the basal area, average basal width (diameter of a circle with the equivalent area), and major and minor basal axes. A 3D basal surface calculated from the edifice outline by inverse distance weighting (IDW) is then used to

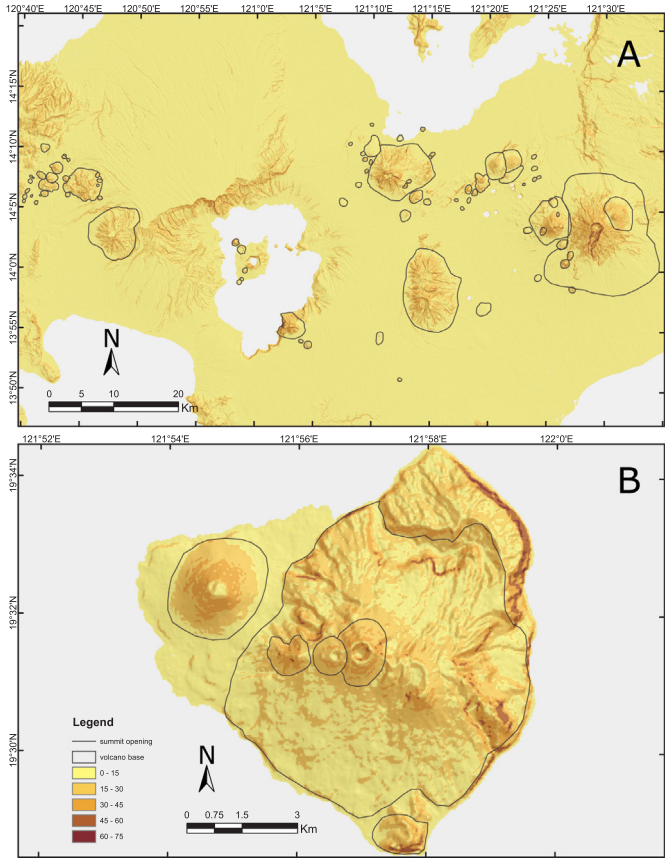

Fig. 2. SRTM 30 m DEM-derived slope map showing examples of single and overlapping volcano edifice bases. Volcano bases are drawn as black polygons.

estimate edifice height and volume. 50-m elevation contours and a summit region, where the edifice starts flattening out, are generated from the DEM. For each closed elevation contour, two dimensionless indexes are computed that give an estimate of the elongation (ellipticity index) and complexity (irregularity index) (Grosse et al., 2012). The DEM-derived slope map is used to compute average slope values for the whole edifice, the summit region and the edifice flank (excluding the summit region), the latter also separated into lower and main flanks (below and above the lowermost closed elevation contour, respectively). Small closed contours produced by topographic highs or lows are counted as secondary peaks or depressions, which can estimate terrain roughness and are related to the number of secondary vents and erosional features (Grosse et al., 2012).

For edifices with delineated summit craters, the crater is either contained within the summit region or is used directly as the summit region if there is no significant slope decrease or no closed contour below the crater outline. In the latter case, we used the crater width rather than the summit width for calculating the summit width/basal width ratio. MORVOLC also computes additional crater-related parameters: area, average width, major axis length and azimuth, depth, volume of the depression, ellipticity index, irregularity index, and average slope within the crater. Further descriptions of the parameters used are given in the supplementary data on Philippine volcanoes morphometry and for further details on MORVOLC, see Grosse et al. (2012, 2014).

3.3. Morphometric classification

MORVOLC generates a multidimensional morphometric dataset with continuous and correlated variables; therefore, we used principal component analysis (PCA) and clustering analysis to classify the morphometry of the volcanoes. PCA is a preprocessing step before performing clustering analysis used to reduce the dimensions of the data to a few uncorrelated continuous variables or principal components (PC) containing a large part of the total variance of the dataset (e.g., Jolliffe, 2002). We selected 15 morphometric variables with data for all volcanic edifices to perform the PCA (Table 1).

Volcano edifices were then classified based on their morphometry by performing hierarchical clustering with the first four PC (HCPC). Clustering is an unsupervised method for partitioning a dataset into groups or clusters. This method requires a definition for distance and an agglomeration criterion (Köhn and Hubert, 2015). We used the Manhattan distance and Ward's criterion, which decomposes the total variance into between- and within-group variance. This method consists of aggregating two clusters such that the growth of within-group variance is minimised, implying homogeneity within a cluster. The hierarchy is represented by a dendrogram indexed by the gain of within-group variance.

To evaluate goodness of clustering, we examined the within-cluster variation. To measure how well separated a cluster is from other clusters, we used distances between cluster centres and the pairwise minimum distances between objects in different clusters. Silhouette plots show how well an observation is clustered, and allow estimating the average distance between clusters (Jolliffe, 2002).

3.4. Spatial distribution and alignment of volcanic centres in volcanic fields

The spatial distribution and alignment of volcanic centres within volcanic fields and the general shape of the volcanic field itself provide important constraints for understanding controls on volcano evolution (Condit and Connor, 1996; Le Corvec et al., 2013). We used the Matlab Geological Image Analysis Software (GIAS) code developed by Beggan and Hamilton (2010) to evaluate the spatial distribution of the volcanic centres in each volcanic field, compared to that expected for a Poisson nearest-neighbour (PNN) statistical model (Clark and Evans, 1954). The code determines the mean nearest neighbour distances for the observed (R_0) and expected (R_e) distribution, and obtains the population-dependent R_0 and R_e (Baloga et al., 2007). The population density is calculated using a convex hull generated by connecting the outermost points of the population (Hamilton et al., 2010; Le Corvec et al., 2013) divided by the number of volcanoes per volcanic field. R values, which compare the spatial distribution of the natural system with the Poisson model, and c values, which assess the significance of the comparison, are plotted with 2σ confidence intervals to overcome the sample-dependent bias and properly assess the suitability of the PNN analysis. The shape of volcanic fields, from sub-circular to low eccentricity ellipses, can provide important information on the nature and behaviour of the source and the magma plumbing system (Condit and Connor, 1996; Le Corvec et al., 2013). Shapes are determined by various processes, including the duration of volcanic activity and the geometry of the source (Le Corvec et al., 2013). The GIAS code describes the shapes of volcanic fields by fitting a minimum-area ellipse around the volcanic centres and defining the axial ratio of the ellipse, and volcanic field orientation by the azimuth of the major axis of the ellipse.

A Matlab three-point alignment code was then used to identify groups of at least three volcanic centres that form a straight line within certain length and thickness tolerances for the lineament (Le Corvec et al., 2013). To take into account the fact that volcanic fields often cover a large area but have a small mean distance between volcanic centres due to, for example, magma propagating through new fractures or reactivated pre-existing structures (Le Corvec et al., 2013; Wadge and Cross, 1988; Connor et al., 1992; Baloga et al., 2007; Bleacher et al., 2009), the code uses density-defined maximum distances between volcanic centres for the length tolerance. The code then generates a list of alignment azimuths of lines formed by at least three volcanoes, for each volcanic field. These azimuths are then plotted on a rose diagram to visualise the preferred alignments.

Table 1
Morphometric parameters used for the principal component (PC) and clustering analyses. The percentages correspond to the amount of variation explained by each of the principal components. Bold values indicate the largest contribution of each variable to the first four PCs. Blue is a positive contribution, red is a negative contribution, with darker colours indicating larger contributions.

Morphometric Parameters			PC1	PC2	PC3	PC4
			52.4%	17.5%	9.1%	7.8%
Size	Base	Area	**0.91**	0.03	−0.24	0.24
		Average width	**0.96**	0.04	−0.22	0.03
		Maximum axis	**0.95**	0.04	−0.24	0.05
	Summit	Area	**0.82**	−0.07	0.38	0.08
		Average width	**0.88**	−0.13	0.39	0.01
		Maximum axis	**0.74**	−0.13	0.55	−0.20
	Overall	Edifice height	**0.82**	0.29	−0.16	−0.05
		Edifice volume	**0.89**	0.04	−0.14	0.26
Plan Shape	Irregularity	Number of secondary peak	**0.87**	0.03	−0.25	0.21
		Average irregularity index of main elevation curves	**0.80**	−0.13	0.33	−0.25
	Elongation	Average ellipticity index of main elevation curves	0.29	0.05	−0.05	**−0.79**
Truncation		Summit width/basal width ratio	−0.21	−0.44	**0.52**	0.44
Profile Shape		Height/basal width ratio	−0.35	**0.84**	0.T22	0.22
	Slope	Mean slope of whole edifice	−0.10	**0.92**	0.24	0.03
		Standard deviation of slope of whole edifice	0.28	**0.86**	0.12	−0.04

3.5. Geochemistry

To obtain a reasonably complete database of geochemical analyses for Philippine volcanoes, we used the GEOROC database (http://georoc.mpch-mainz.gwdg.de/georoc/Start.asp). The database was queried by longitude and latitude, and all of the relevant volcanic whole-rock analyses were selected for download. The analyses were matched to volcanoes in our database using the sample descriptions and location maps in the original articles. Only analyses where a complete set of major elements was available were considered. This yielded a mean of 8.2 analyses per volcano from a total of 76 volcanoes. A full list of references can be found in the supplementary material. For consistency, all FeO and Fe_2O_3 analyses were converted to the equivalent as Fe_2O_3 only, and major elements were normalised to 100%.

4. Results

4.1. Database of Philippine volcanoes

This work presents a database consisting of the volcano edifice outlines and their morphometric parameters and descriptions (supplementary data). The data for selected volcanoes is listed in Table 2, and the 731 edifice outlines are shown in Fig. 1. Volcanoes are organized geographically into nine volcanic regions and eight volcanic fields, with high densities of small cones (≤7 km^3 volume) with or without larger volcanoes (Fig. 1). The volcanoes delineated in this work were cross-checked with the existing list of volcanoes of the Philippine Institute of Volcanology and Seismology (2008), but also includes many that are not on that list, particularly smaller edifices. Although we have endeavoured to identify all volcanoes in a systematic fashion, we acknowledge that some volcanoes may have been left out and some entries may have been misidentified. Hence, we anticipate that the current database will improve with time.

4.2. Morphometric classification

The volcanic edifices were classified using hierarchical classification based on the first four principal components obtained from 15 of the morphometric parameters generated by MORVOLC (Table 1). The selected parameters describe the base, summit, and overall size, plan (irregularity and ellipticity or elongation) and profile (height/basal width ratio and mean slope) shapes, number of secondary peaks, and truncation (summit width/basal width ratio). For volcanoes with delineated craters, we use the width of the crater as the summit width.

The size parameters are strongly positively correlated (blue circles in Fig. 3A) with each other and with edifice irregularity and number of peaks, and weakly positively correlated with elongation. Edifice size is weakly negatively correlated (red circles) with truncation and mean slope. Elongation, truncation and mean slope are weakly correlated with each other (Fig. 3A).

We use the first four PC based on the Kaiser-Guttman rule, which retains PC with eigenvalues greater than 1. ~87% of the information or variance contained in the data are retained by the first four PC (Table 1). The positively correlated size and plan-shape irregularity variables contribute mostly to PC1, the height/basal width ratio and mean slope (i.e., steepness) contribute mostly to PC2, truncation contributes almost equally to PC3 and PC4, and elongation contributes mostly to PC4 (Table 1; Fig. 3A).

Based on the morphometric information captured by the four PCs, hierarchical clustering of 711 volcano edifices (excluding 20 small edifices with delineated craters that lack closed elevation contours, and which thus lack values for their ellipticity and irregularity indices) was implemented to classify Philippine volcanoes into groups of self-similar edifices. The hierarchical clustering produced four clusters. The edifices in clusters 1 (373 edifices) and 2 (258 edifices) are small (low PC1 values; Fig. 3C). Those in cluster 1 have low PC2 values and hence are classified as small flat cones, whereas those in cluster 2 have high PC2 values and are classified as small steep cones (Fig. 3C). Cluster 3

Table 2
Morphometric parameters and classification of selected Philippine volcanoes. The complete list of volcanoes with their classification and all computed morphometric parameters and their descriptions is presented in the Supplementary Data.

Volcano		Location		Size			Plan shape		Profile shape		Slope	Summit crater/caldera	
Name	Field/Region[a]	East	North	Height	Base Width	Volume	Ellipticity Index (mean)	Irregularity Index (mean)	H/BW[b]	SW/BW[b]	Mean Slope	Depth	Crater Width
		UTM		*m*	*km*	*km³*	*dimensionless*		*dimensionless*		*degrees*	*m*	*km*
Small flat cones													
Anilao Hill	Macolod VF	303,109	1,538,433	81	1.46	0.03	1.21	1.02	0.056	0.209	6		
Musuan	Maramag VF	728,149	871,263	288	2.46	0.39	1.21	1.04	0.117	0.065	12		
Tapul	Basilan VF	267,979	634,023	452	5.9	3.15	1.97	1.31	0.077	0.051	10		
	Range			*16–721*	*0.2–7.8*	*0–6.2*	*1.1–5.8*	*1–2.3*	*0.012–0.169*	*0.024–1.000*	*3–21*	*11.5–112.9*	*0.20–1.19*
	Mean			*125*	*1.4*	*0.2*	*1.8*	*1.1*	*0.100*	*0.376*	*13*	*28.3*	*0.48*
Small steep cones													
Banahao de Lucban	Macolod VF	339,439	1,556,643	554	4.6	1.64	1.26	1.04	0.120	0.047	19		
Basco	Batanes VR	396,859	2,263,443	971	4.9	5.34	1.69	1.32	0.200	0.062	25		
Biliran	East Visayas VR	651,979	1,290,243	953	7.5	9.0	2.00	1.37	0.126	0.052	17		
Buddajo with crater	Basilan VF	284,749	665,163	332	1.85	0.25	1.17	1.06	0.179	0.388	22	37	0.47
Hibok-hibok	North Mindanao VR	684,079	1,017,333	923	5.8	6.3	1.64	1.19	0.159	0.125	21		
Lignon Hill	Bicol VR	578,989	1,455,033	123	0.80	0.02	1.48	1.05	0.154	0.403	17		
San Cristobal	Macolod VF	330,109	1,555,413	955	6.5	6.8	1.65	1.15	0.148	0.092	16		
Smith	Batanes VR	385,819	2,160,723	582	2.69	0.93	1.13	1.02	0.216	0.150	22		
Vulcan with crater	North Mindanao VR	681,109	1,018,923	298	1.47	0.18	1.39	1.03	0.202		28	22	0.29
	Range			*53–971*	*0.4–7.5*	*0–9*	*1.1–4.9*	*1–1.8*	*0.081–0.323*	*0.013–0.835*	*14–37*	*6.2–116.6*	*0.23–1.42*
	Mean			*260*	*1.6*	*0.4*	*1.8*	*1.1*	*0.174*	*0.265*	*22*	*34.4*	*0.44*
Large cones													
Apo	South Mindanao VR	750,889	772,953	1693	22	164	1.88	1.31	0.076	0.141	20		
Arayat	Western Luzon VR	257,449	1,682,313	998	9	12.0	1.57	1.33	0.117	0.102	13		
Babuyan Claro with crater	Batanes VR	390,049	2,159,253	952	7.8	12.3	2.29	1.32	0.122	0.328	18	126	0.54
Banahaw	Macolod VF	337,159	1,555,683	1750	17	75	1.74	1.62	0.100	0.096	13		
Iriga	Bicol VR	548,809	1,487,883	1039	9.1	11.9	2.02	1.39	0.114	0.043	12		
Kanlaon with crater	Negros VR	514,249	1,150,713	2099	23	178	2.13	1.57	0.092		15	89	0.47
Leonard Massif with crater	South Mindanao VR	838,129	810,123	940	22	124	1.95	1.50	0.043		20	126	2.32
Makiling	Macolod VF	304,429	1,563,363	910	9.1	13.0	1.85	1.58	0.101	0.112	16		
Malindig	South Luzon VR	393,049	1,464,003	1080	8.3	13.6	1.86	1.38	0.130	0.118	17		
Mambajao	North Mindanao VR	689,779	1,015,053	1330	10.4	29	1.89	1.59	0.128	0.151	21		
Matutum	South Mindanao VR	729,739	703,533	1482	17	42	1.47	1.26	0.087	0.014	11		
Mayon	Bicol VR	574,249	1,465,503	2313	17	70	1.16	1.13	0.134	0.002	10		
Pinatubo with crater	Western Luzon VR	217,489	1,677,663	1014	25	86	4.04	1.46	0.041		16	389	2.59
Samat with crater	Western Luzon VR	226,849	1,606,653	1365	24	110	1.46	2.81	0.057		12	535	3.76
Sugarloaf	Zamboanga VF	528,469	883,143	687	6.3	4	3.55	1.59	0.109	0.069	22		
Talomo	South Mindanao VR	755,899	778,923	1292	24	61	3.49	1.64	0.055	0.110	11		
	Range			*59–2313*	*1.6–26*	0.15–178	*1.2–12.5*	*1–5.1*	*0.007–0.162*	*0.002–0.580*	*3–28*	*2–58*	*0.00–0.06*
	Mean			*842.1*	*11.2*	28.8	*2.8*	*1.7*	*0.081*	*0.189*	*15*	*22.7*	*0.02*
Massifs													
Balatukan	North Mindanao VR	717,379	967,743	1869	34	479	3.24	3.19	0.055	0.261	18		
Bao	East Visayas VR	690,349	1,228,023	1109	33	185	3.22	1.75	0.034	0.055	14		
Cuernos de Negros	Negros VR	519,349	1,021,743	1740	35	343	2.49	3.81	0.050	0.234	14		
Kilatungan	North Mindanao VR	698,629	879,783	1935	37	363	2.37	2.12	0.053	0.084	12		
Natib	Western Luzon VR	220,129	1,628,073	1230	28	124	2.27	3.47	0.044	0.140	11		
Parker with crater	South Mindanao VR	708,739	672,393	1234	28	155	2.46	1.52	0.045		16	340	2.82
Ragang	North Mindanao VR	666,199	850,443	1618	38	265	2.23	2.16	0.042	0.106	13		
	Range			*1012–2175*	*18.6–51*	*76–675*	*1.9–4.2*	*1.5–4.9*	*0.031–0.062*	*0.034–0.428*	*11–22*	*51.3–340.2*	*0.98–2.82*
	Mean			*1533*	*33*	*267*	*2.8*	*2.8*	*0.048*	*0.180*	*15*	*195.8*	*1.9*

[a] VF: volcanic field, VR: volcanic region.
[b] H: height, BW: basal width, SW: summit width.

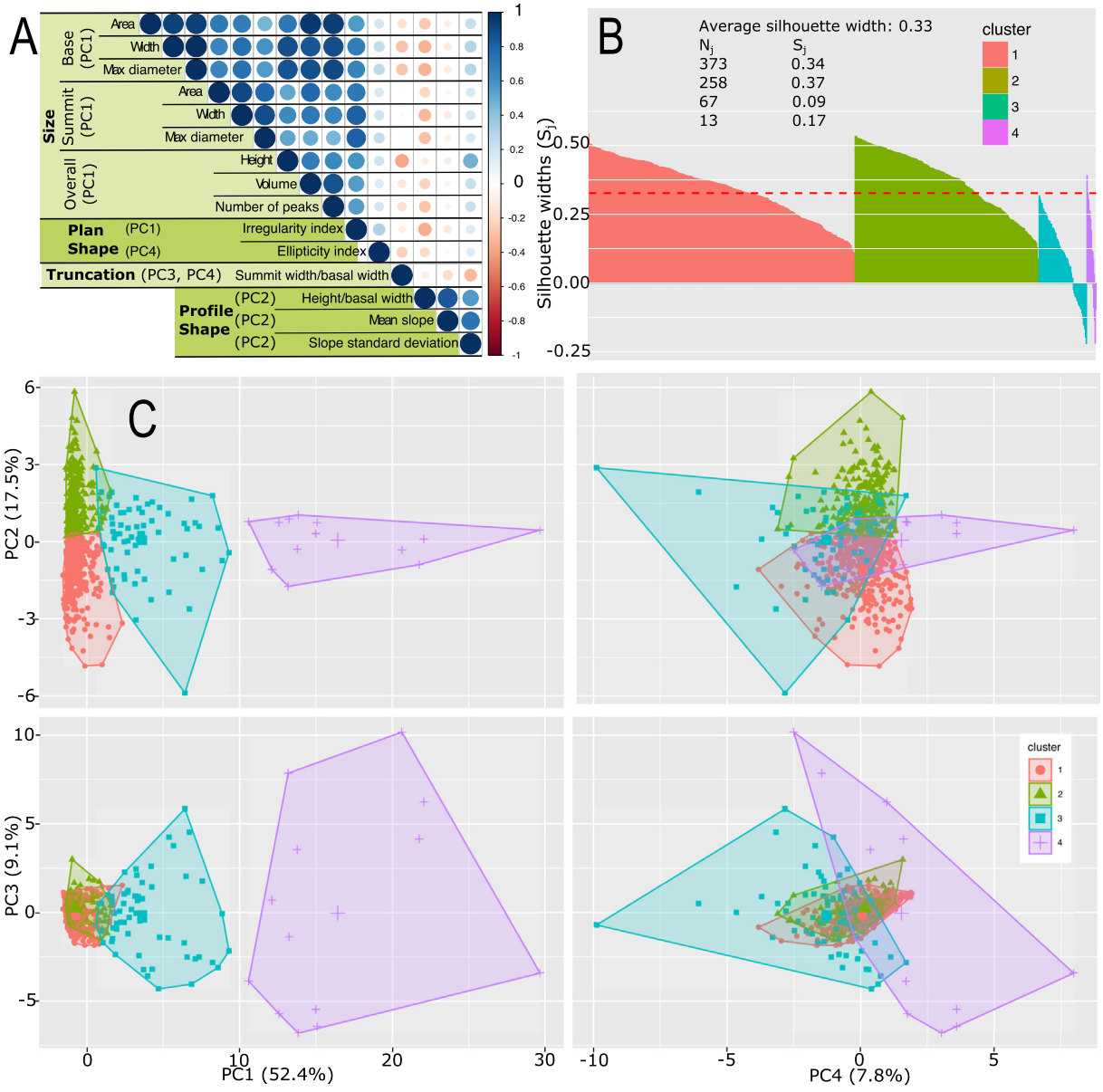

Fig. 3. Results of principal component analysis and hierarchical classification by principal components. A Correlation plot for the 15 morphometric parameters used. Colour intensity and the size of the circles are proportional to the correlation coefficient ranging from −1 to +1. B Silhouette plot showing the performance of the clustering—a higher average silhouette width is better, and negative silhouettes represent volcanoes that may not be in the correct cluster. N_j is the number of edifices and S_j is the silhouette width in each cluster, j. C Hierarchical clustering based on the first four PC, showing PC1 (size, irregularity, and number of peaks) versus PC2 (steepness: height/basal width ratio and slope), PC3 (irregularity, truncation, and size of summit area), and PC4 (elongation and truncation). Clusters 1, 2, 3, and 4 are interpreted to be small flat cones, small steep cones, large cones, and massifs, respectively.

contains 67 edifices with intermediate PC1 values (Fig. 3C), and are classified as large cones. Cluster 4 consists of 13 edifices with high PC1 values (Fig. 3C) and are classified as massifs. There is no clear distinction between the clusters using PC3 and PC4 (Fig. 3C), although the large cones tend to have lower PC4 values than the massifs. Table 2 lists the general morphometric characteristics of each cluster.

Small flat cones have a mean height of 125 m (range = 16–721 m), a mean volume of 0.2 km^3 (<6.2 km^3), and a mean slope of 13° (3°–21°). They are often distributed across the slopes of larger volcanoes, including Makaturing, Maramag, and Ragang, and can be found in the Basilan, Upi, Zamboanga, and Lanao volcanic fields. Small steep cones have a mean height of 260 m (53–971 m), a mean volume of 0.4 km^3 (<9 km^3), and a mean slope of 22° (14°–37°). They can be found in volcanic fields of Lanao, Macolod, and Zamboanga, and on the slopes of large volcanoes such as Labo, Makaturing, Maramag, Parker, Camiguin de Babuyanes, Mandalagan, and those on Camiguin Island in Mindanao. Large cones have a mean height of 842 m (59–2314 m), a mean volume of 29 km^3 (0.15–178 km^3), and a mean slope of 15° (3°–28°). In this group are many of the more well-known active and potentially active volcanoes (e.g., Mayon, Iriga, Kanlaon, Matutum, and Apo). The massifs are large, irregular, and have more peaks than most of the smaller edifices, with a mean height of 1533 m (1012–2175 m), a mean volume of 267 km^3 (76–675 km^3), and a mean slope of 15° (11°–22°). Massifs include Cuernos de Negros, Balatukan, Malindang, Kilatungan, Kitanglad, Parker, and Ragang. Large cones and massifs are mostly found in Western Luzon, Bicol, Eastern Visayas, Negros, and North and South Mindanao.

Average inter- and intra-cluster distances and the Dunn-index suggest that the clusters are well separated from each other. Using the distance of each point in a cluster to neighbouring clusters, most volcanoes in clusters 1 and 2 are well separated from the other clusters (Fig. 3B). Negative values for some volcanoes in clusters 3 and 4 suggest a lower separability and possible misclassification.

Since cone morphology can be influenced by substrate topography (Tibaldi, 1995; Corazzato and Tibaldi, 2006), we considered

Table 3
Results of the spatial statistical, shape, and alignment analyses for each of the Philippine volcanic fields.

		Volcanic Fields							
		Basilan	Labo	Lanao	Macolod	Makaturing	Maramag	Upi	Zamboanga
Measured nearest neighbour properties	Number of volcanic centres (N)	148	19	50	84	36	78	17	40
	Number of Objects in Convex Hull	138	13	39	74	28	68	13	32
	Convex Hull Area (km^2)	10,617	126	1462	2234	245	2776	204	1959
	Population Density ($\times 10^{-3}\,km^{-2}$)	13	103	27	33	114	24	64	16
	Minimum NN Distance (km)	0.36	1.0	0.6	0.3	0.4	0.5	0.4	0.8
	Maximum NN Distance (km)	16	2	4	10	3	8	5	11
	Mean NN Distance (km)	2.0	1.3	1.8	2.0	1.2	1.9	2.3	3.0
	Standard Deviation (2σ) (km)	4.43	0.61	1.99	3.86	1.20	3.25	3.45	4.68
	Skewness	3.35	0.79	0.76	2.50	1.75	2.53	0.31	1.52
	Kurtosis	17.08	2.30	2.54	9.15	8.15	9.72	1.65	4.97
Nearest neighbour results relative to the Poisson model	Poisson Expected Mean NN Distance (km)	4	2	3	3	1	3	2	4
	R	0.46	0.84	0.58	0.73	0.84	0.58	1.14	0.76
	Ideal R	1.04	1.15	1.08	1.06	1.09	1.06	1.15	1.08
	R Threshold ($\pm 2\sigma$)	0.94–1.14	0.75–1.55	0.87–1.28	0.91–1.20	0.85–1.34	0.91–1.21	0.75–1.55	0.86–1.30
	C	−12.16	−1.09	−5.03	−4.49	−1.67	−6.60	0.94	−2.65
	Ideal C	0.84	0.97	0.88	0.87	0.89	0.87	0.97	0.88
	C Threshold ($\pm 2\sigma$)	−1.31–3.0	−1.62–3.56	−1.46–3.23	−1.38–3.12	−1.48–3.27	−1.40–3.15	−1.62–3.56	−1.46–3.23
Spatial Distribution		Clustered Significant	Random Insignificant	Clustered Significant	Clustered Significant	Clustered Significant	Clustered Significant	Random Insignificant	Clustered Significant
Alignment analysis	Maximum distance for the generation of lineaments (m)	9000	3800	7200	6700	3500	7400	5000	8500
	Number of lineaments	196	3	17	101	7	56	1	9
Shape analysis	Short axis ellipse (MinVolEllipse) (m)	123,039	14,514	44,055	48,650	37,920	53,961	16,690	45,695
	Long axis ellipse (MinVolEllipse) (m)	233,600	18,608	70,505	110,616	61,468	72,982	37,515	86,490
	Short Axis/Long Axis (MinVolEllipse)	0.53	0.78	0.62	0.44	0.62	0.74	0.44	0.53
	Azimuth	57°	85°	70°	90°	84°	320°	335°	48°

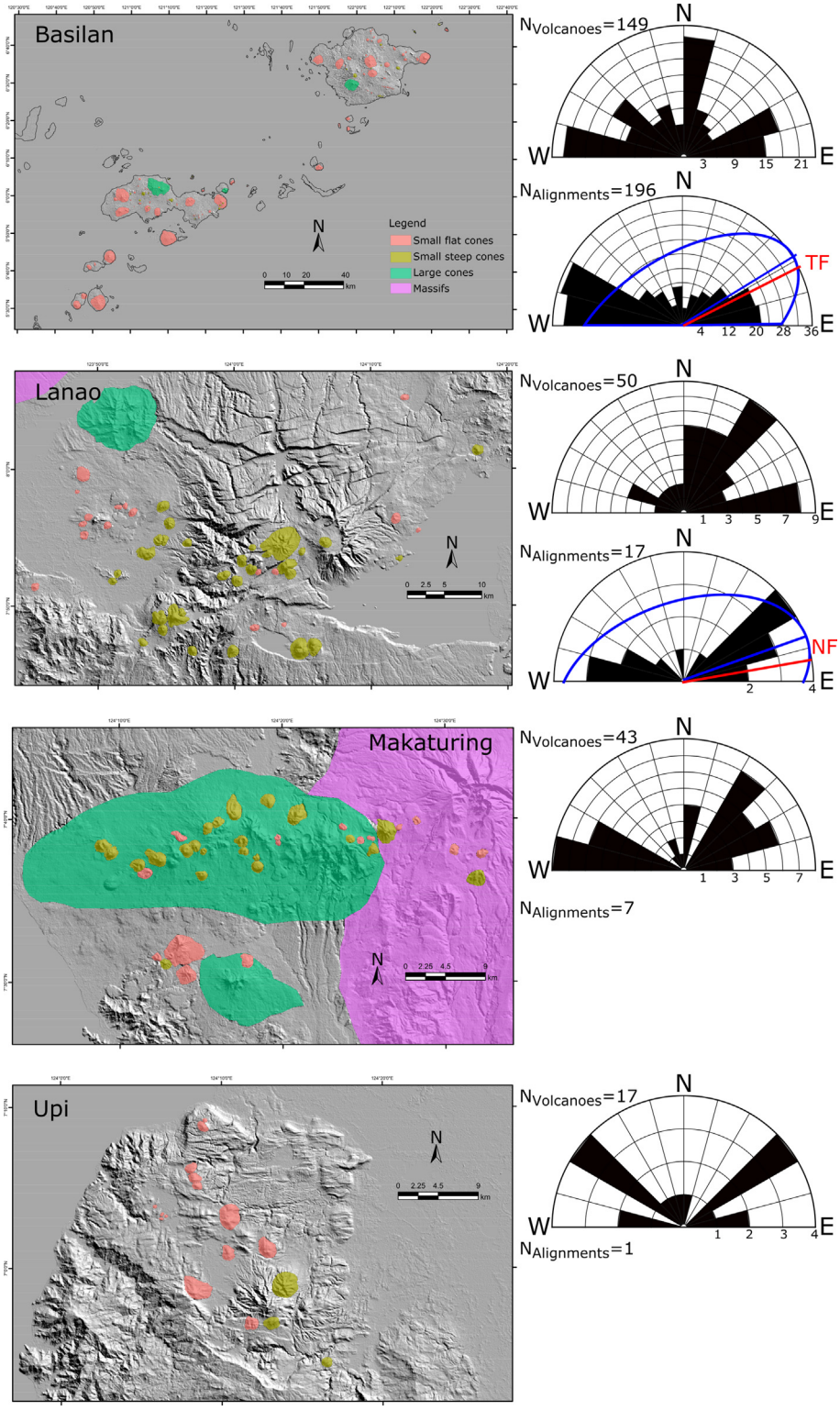

Fig. 4. Distribution and classification of volcano edifices in Basilan, Lanao, Makaturing, Upi, Labo, Macolod, Maramag, and Zamboanga volcanic fields *(left)*. The number of volcanoes ($N_{Volcanoes}$) and alignments ($N_{Alignments}$) formed by at least three volcanic centres are given. *Upper rose diagrams* show the volcano base elongation azimuths; *lower rose diagrams* show preferred alignment directions for volcanic fields with more than 10 alignments; *blue half ellipses* and *blue lines* show the ellipticity and the long axis directions of the volcanic fields; and the *red lines* are the orientation of the main faults in the fields: in Basilan, this represents the Sulu Trench as drawn by Aurelio (2000) and Aurelio and Pena (2002), in Lanao, these are the ~80° striking normal faults that can be seen in the SRTM DEM , and in Macolod, these are the north–south strike–slip faults and ~70° rift faults (Vogel et al., 2006; Lagmay and Valdivia, 2006).

the effects of buttressing on parasitic and overlapping edifices. Parasitic cones are either small steep or small flat cones, and tend to be slightly steeper than non-parasitic cones, although there is a large overlap in their mean slopes. There is no difference in the values of the other morphometric parameters between parasitic and non-parasitic cones. Some large cones and massifs overlap, but buttressing does not seem to affect their morphometric parameters significantly.

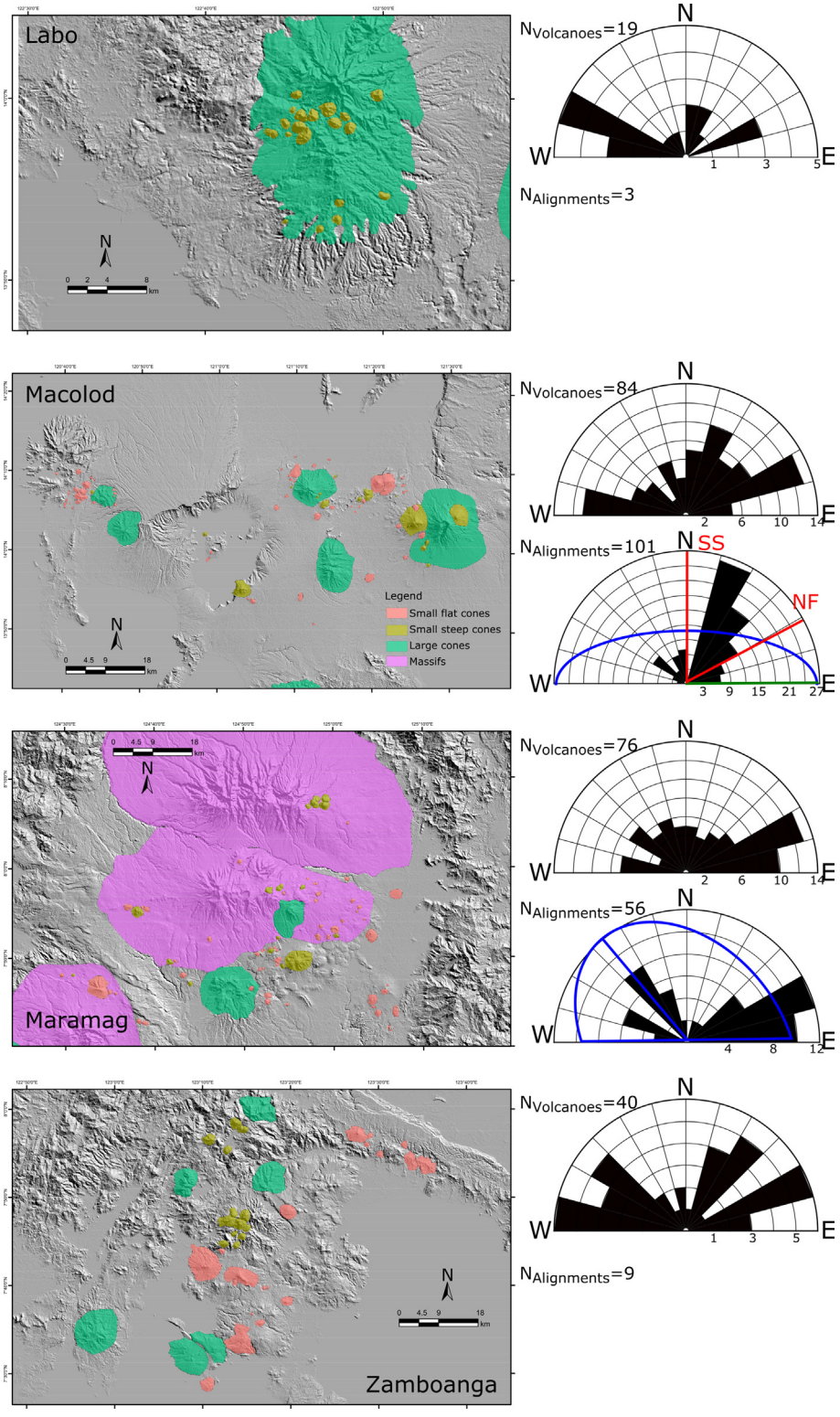

Fig. 4 (*continued*).

4.3. Spatial distribution and alignment of volcanoes

Table 3 lists the results of applying Poisson Nearest-Neighbour analysis to the eight volcanic fields of the Philippines. Basilan, Lanao, Macolod, Makaturing, Maramag, and Zamboanga volcanic fields have c values outside the $\pm 2\sigma$ significance level and R values less than -2σ, which means they are clustered relative to a Poisson distribution. Labo and Upi volcanic fields have c values outside the $\pm 2\sigma$ significance level and R greater than $+2\sigma$, which means they are dispersed.

Considering the volcano density and the relationships established using the global database of monogenetic volcanic fields by Le Corvec et al. (2013), the maximum distances needed for the generation of lineaments for the volcanic fields are 3.5–9.0 km (Table 3). We used a width tolerance of 100 m for all the volcanic fields, considering the

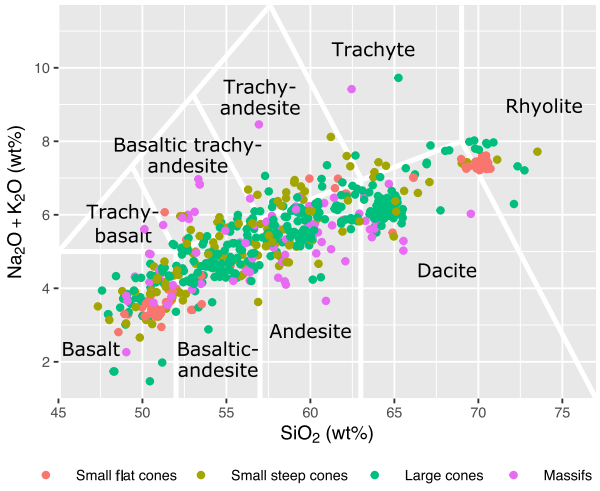

Fig. 5. Total alkali–silica plot after Le Maitre et al. (2005)

uncertainties due to the locations of the volcanic centres relative to the original vents and the width of dike swarms and zones. Additional uncertainty comes from the lack of bathymetric data, for example, in Basilan, where submarine volcanoes that would reduce the distance between neighbouring volcanoes are excluded. This analysis was run for the volcanic fields but not for volcanic regions because larger edifices are fewer and farther apart.

A three-point MATLAB script (Le Corvec, personal communication) was used to automatically extract the different alignments of the volcanoes within volcanic fields and plot the direction of the alignments on a rose diagram (Fig. 4). Fig. 4 also shows half ellipse shapes of the volcanic fields, the directions of the long axis of the ellipse, and the directions of some of the faults in Basilan, Lanao, and Macolod volcanic fields that can be seen in the SRTM DEM or have been noted in previous studies (Aurelio, 2000; Aurelio and Pena, 2002; Vogel et al., 2006; Lagmay and Valdivia, 2006). The minimum-area ellipses that fit the fields are mostly elongated, with short-to-long axis ratios of 0.28–0.78 (Table 3). We only analysed the spatial distribution of the four fields with more than 10 alignments. Basilan and Macolod volcanic fields have one preferred alignment orientation, whereas Lanao and Maramag volcanic fields have two. Basilan, Macolod, and Lanao have preferred alignment orientations that coincide with the directions of their dominant tectonic structures (Fig. 4). All four volcanic fields with more than 10 alignments have preferred alignment directions that also coincide with the orientation of the shape of the field (Table 3; Fig. 4). The elongation azimuths of the edifice bases are roughly parallel to the dominant alignment direction in most of the volcanic fields, although the variation is high (Fig. 4).

4.4. Geochemistry

In general, Philippine volcanoes have compositions that form a single, broad, continuous trend from basalt to rhyolite (Fig. 5); however, by considering each morphometric class separately some patterns do emerge. Individual small flat cones have restricted compositions; these form a bimodal distribution with most volcanoes having either basaltic or dacitic–rhyolitic compositions (Fig. 6A, E). Individual small steep cones tend to have a larger range in SiO_2 (Fig. 6F), suggesting that they have had multiple eruptions. Small steep cones are mostly basaltic and andesitic (Fig. 6B), with very few silicic volcanoes. Large cones are mostly basaltic-andesite to andesite, with some dacitic eruptions (Fig. 6C). Both as a group and individually, massifs have a large range of compositions, although only a few of the samples are dacitic or rhyolitic (Fig. 6D, H). As well as having a large range of SiO_2 contents, massifs show more variability in other elements (e.g., $Na_2O + K_2O$; Fig. 5).

5. Discussion

5.1. Spatial distribution of the different volcano classes

The distribution of the four volcano classes is shown in Fig. 7, Table 2, and the Supplementary Data. Detailed maps with the distribution of small volcanoes in the volcanic fields are shown in Fig. 4. Large cones and massifs are found mostly in the northern and central part of Mindanao up to Negros, and in East Philippines and West Luzon (Fig. 7). The locations of these volcanoes coincide with regions of thicker crust modelled by Parcutela et al. (2020), who related the depth of the Moho to Bouguer gravity anomalies generated from the EGM2008 global model. The middle of Luzon and Bicol–Negros–Panay–Central Mindanao has crust 25–37.5 km thick, compared to the rest of the archipelago that is characterized by crust ~13–25 km thick (Parcutela et al., 2020). Large cones and massifs in the central part of Mindanao are thought to be related to the collision between western and eastern Mindanao at ~5 Ma (Pubellier et al., 1991; Castillo et al., 1999) and between the Zamboanga–Sulu Peninsula (on the west of Mindanao) and the central part of Mindanao (Yumul et al., 2008). There is no correlation between the locations of small cones, whether steep or flat, and the location of thicker crust.

The distribution of the large cones and massifs suggests that the thickness of the crust may influence the evolution of arc volcanoes. For example, Carr (1984) and Farner and Lee (2017) found a relationship between crustal thickness and the chemistry of the magma erupted globally at arc volcanoes and suggested that the thickness of the crust controlled the magma evolution through processes such as fractional crystallisation and crustal assimilation. Thicker crust makes magma more likely to stall during ascent, forming long-lived magma chambers that focus volcanic activity (Karlstrom et al., 2009; Pansino and Taisne, 2019), which could potentially lead to larger edifices. The longer transit times for the magma also lead to more evolved compositions, which would also lead to steeper and taller edifices (Farner and Lee, 2017).

5.2. Evolutionary trends

Fig. 8 shows plots of selected morphometric parameters for all volcanoes, which, combined with the geochemistry (Fig. 9), suggest possible evolutionary trends. The single trend on the total alkali–silica plot (Fig. 5) suggests that the volcanoes share a similar source and that a similar set of magmatic processes operates at each.

Volcanoes initially develop as small cones, either flat or steep; the steepness might relate to the eruptive style. The bimodal distribution and restricted individual compositions of the small flat cones is consistent with them being monogenetic: either basaltic scoria cones or silicic domes (Fig. 6E). Many of these volcanoes have previously been identified as monogenetic, including scoria cones and silicic domes in the Macolod Volcanic Field (Fig. 1; e.g., Förster et al., 1990; Defant et al., 1991; Knittel and Oles, 1994; Vogel et al., 2006), silicic domes in the Central Luzon back arc (Western Luzon Volcanic Region; Fig. 1; e.g., Yumul et al., 2000a), scoria cones on Taal (e.g., Miklius et al., 1991), and monogenetic parasitic cones on Mount Mariveles (e.g., Defant et al., 1991), although a few small flat cones in the Macolod Corridor may be polygenetic (e.g., Knittel and Oles, 1994). Although scoria cones and silicic domes have steep flanks, the flat tops of domes and the relatively large craters of scoria cones lead to large truncation values and low mean slope values for the entire edifices.

Some of the small steep cones also have restricted compositions (Fig. 6F), and some have also previously been identified as monogenetic, including silicic domes and mafic scoria cones in the Macolod Corridor (e.g., Knittel and Oles, 1994; Vogel et al., 2006) and silicic domes in Irosin Caldera (e.g., McDermott et al., 2005); however, many small steep cones have a larger range of compositions, suggesting multiple eruptions and a polygenetic evolution (Fig. 6F). Small steep cones that have previously been shown to be polygenetic include Guinsiliban,

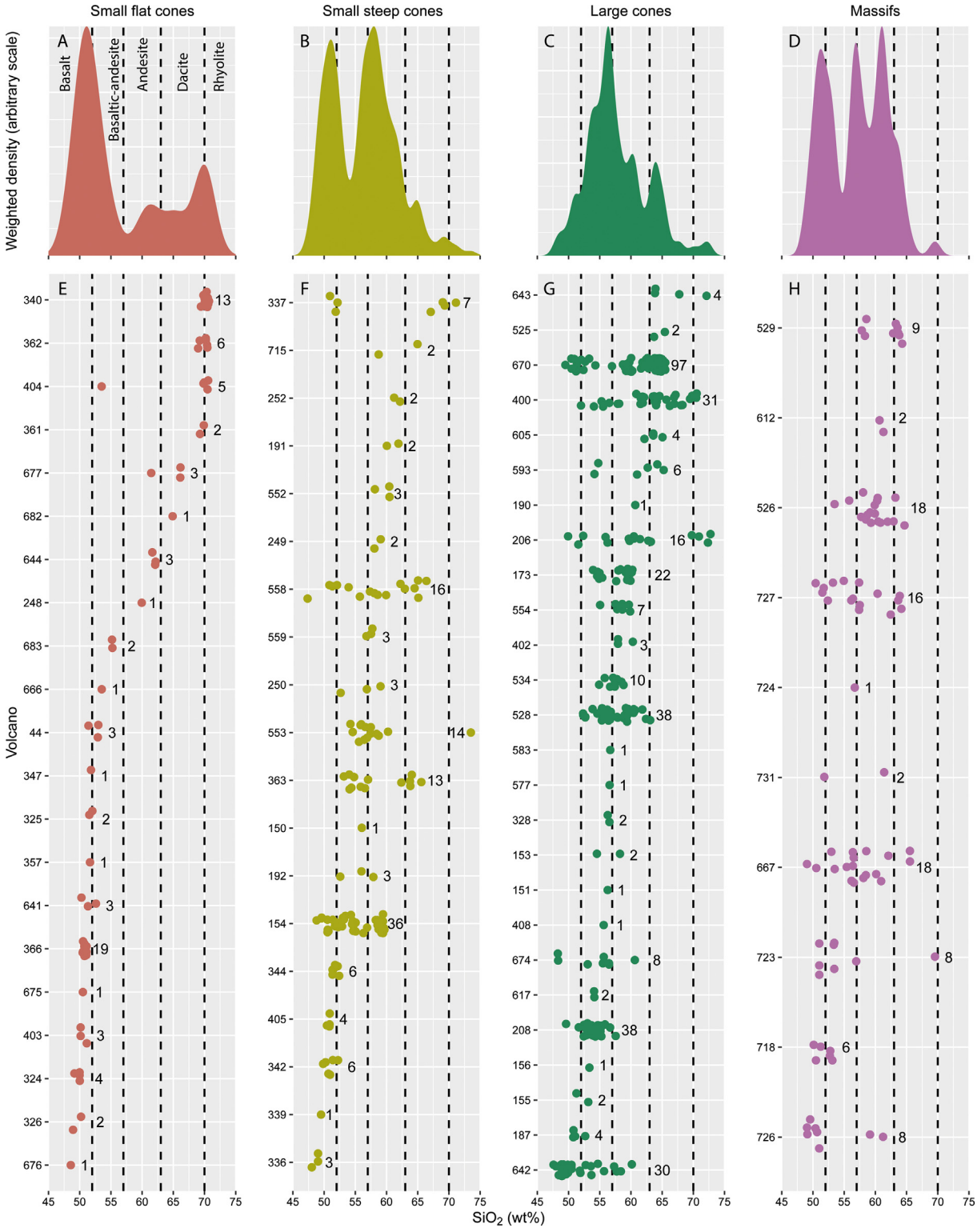

Fig. 6. A–D Probability density plots for the SiO_2 content of rocks from Philippine volcanoes, separated by morphometric class and inversely weighted by the number of analyses from each volcano. E–H SiO_2 content of analyses from each Philippine volcano with available geochemical data, separated by morphometric class and sorted by median SiO_2 content. The ID number of each volcano, as plotted on the y axis, can be found in the Supplementary Data. Numbers to the right of the data are the number of analyses in the database for each volcano.

Uhay, and Hibok-hibok on Camiguin (e.g., Castillo et al., 1999), pre-caldera cones outside Irosin caldera (e.g., Delfin et al., 1993; McDermott et al., 2005), Basco Island in Batanes (e.g., Defant et al., 1990; Sajona et al., 2000), and some cones in the Macolod Corridor (e.g., Defant et al., 1991; Miklius et al., 1991; Knittel and Oles, 1994).

Some of the polygenetic small steep cones may grow steadily vertically and laterally into large cones, and some eventually develop into massifs. The massifs are the largest in terms of volume and basal areas, but reach heights similar to large cones, suggesting that once volcanoes reach a mature threshold they continue growing laterally rather

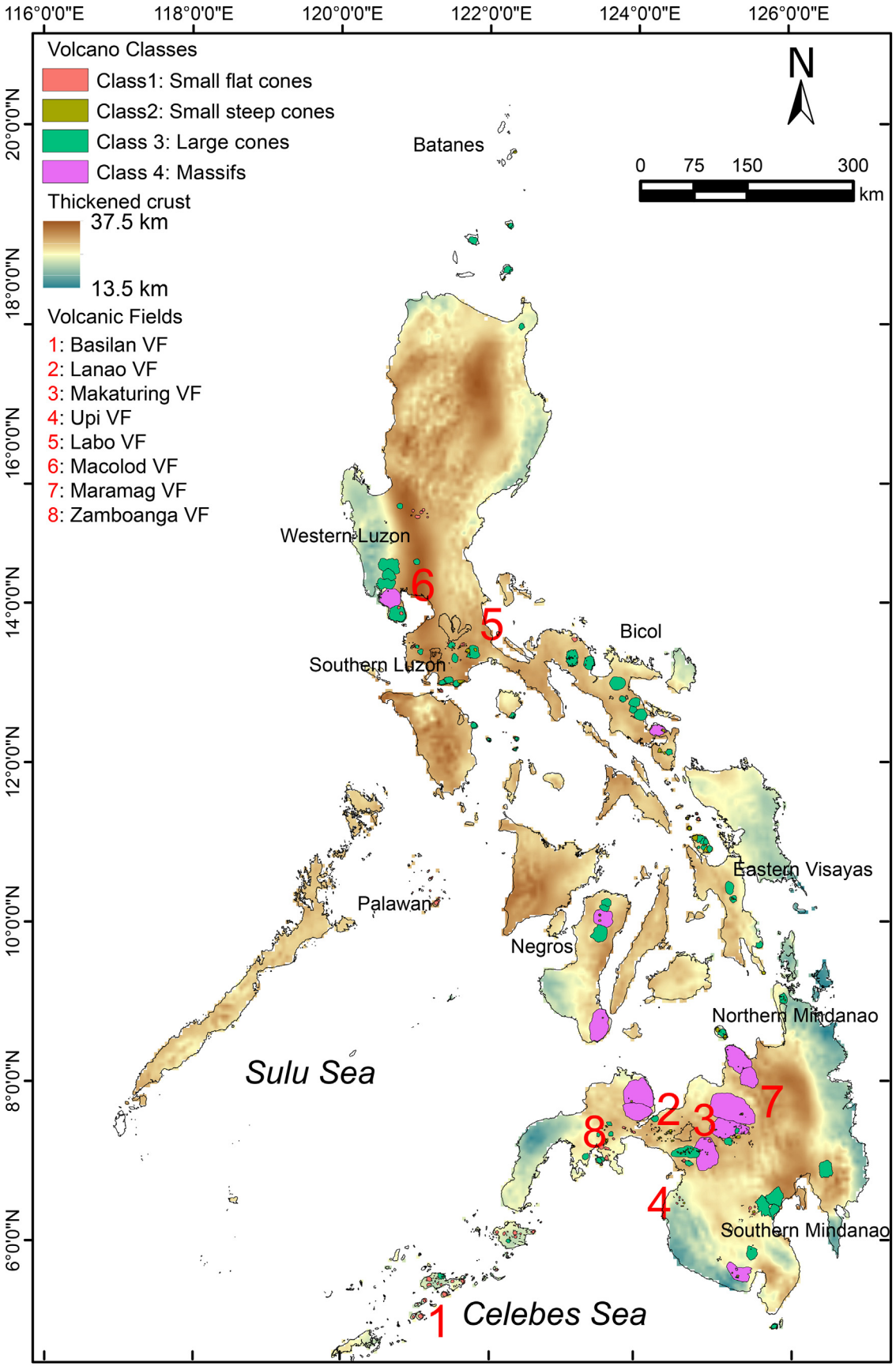

Fig. 7. Philippine volcanoes classified using the hierarchical clustering based on principal components. Crustal thickness is taken from Parcutela et al. (2020). The distribution and classification of small edifices in each volcanic field is shown in Fig. 4.

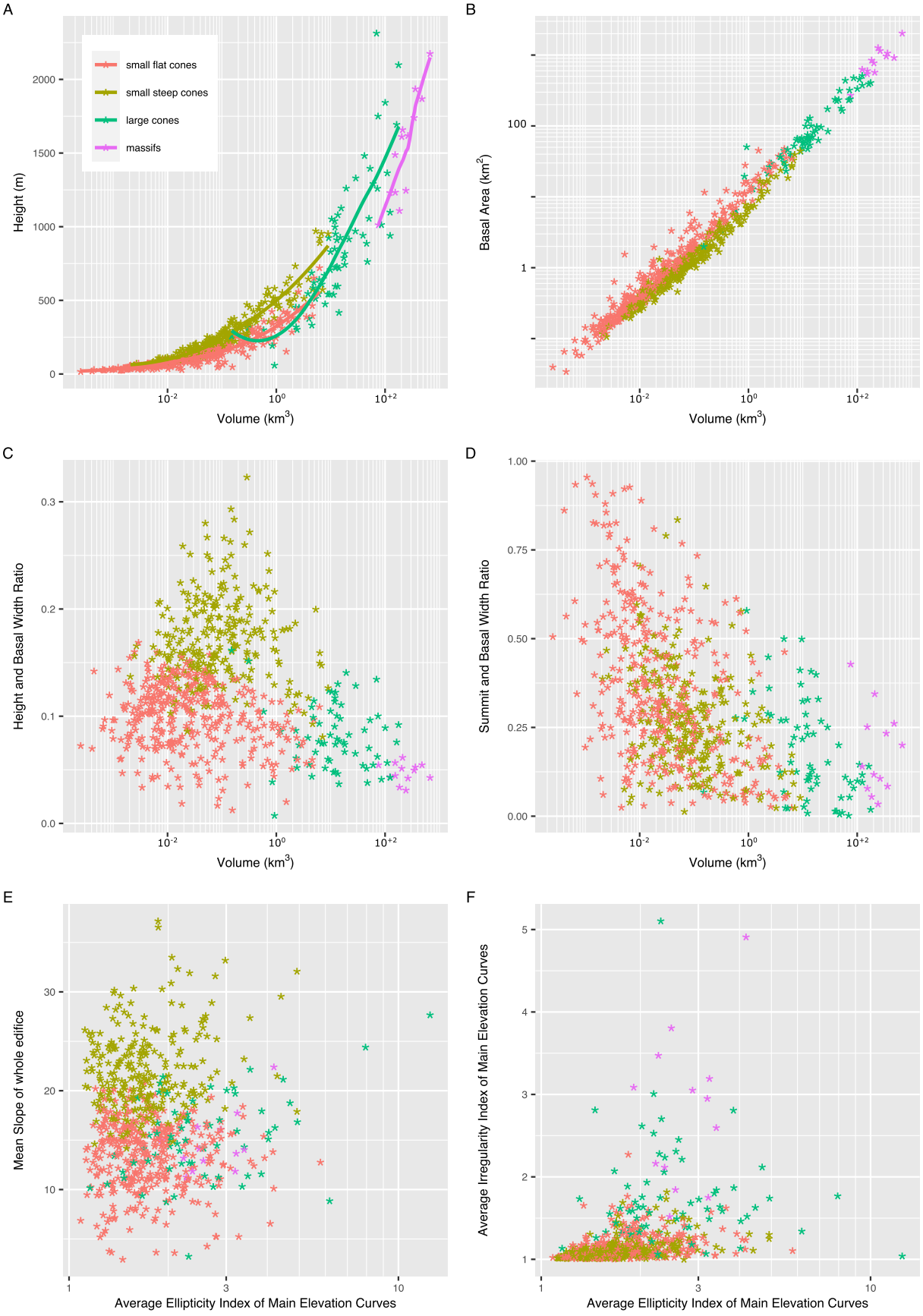

Fig. 8. X–Y scatter plots for different morphometric variables. Regression lines are fitted to the four classes in the volume versus height plot (A).

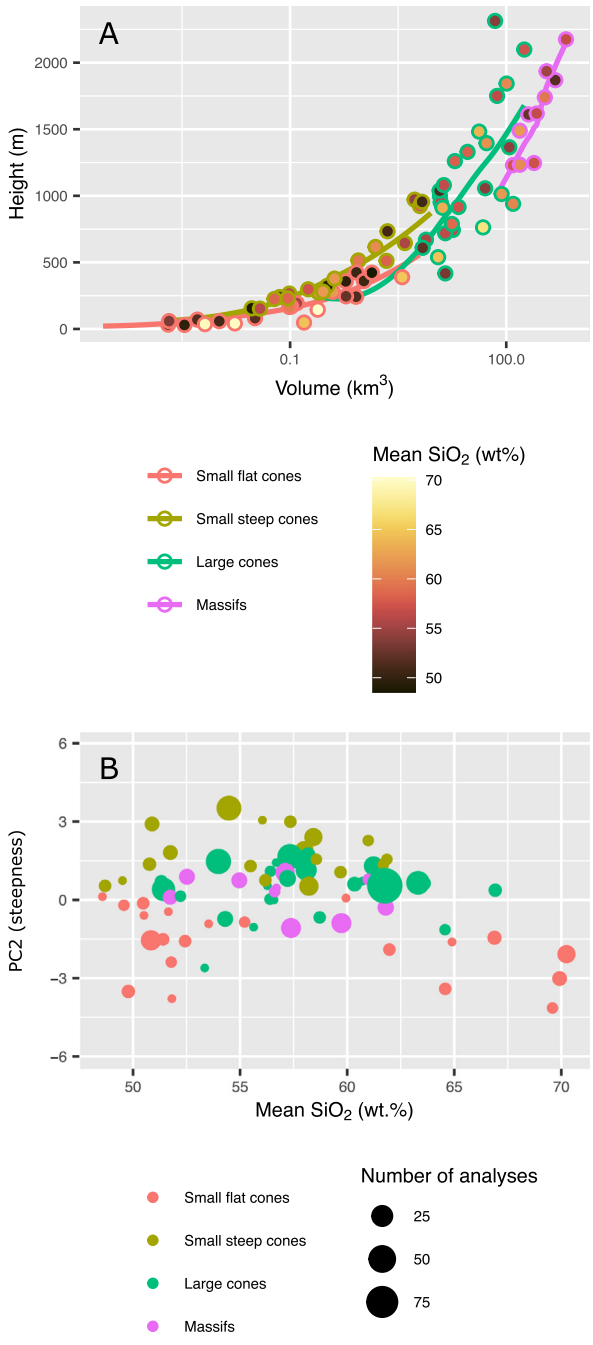

Fig. 9. A Mean SiO_2 contents of the 76 volcanoes for which geochemistry data exists, as a function of their morphometric evolution. Trends as calculated in the regression lines fitted to the four classes in the volume versus height plot in Fig. 8. B Mean SiO_2 content versus principal component 2, which is related to steepness (height/basal width ratio and mean slope).

than vertically (Fig. 8 A–C) (Grosse et al., 2009). Ramalho et al. (2013) suggested that during periods of high magmatic flux, constructional processes dominate the edifice building stages. In order to keep the volcano stable during its growth stages, lateral growth will tend to dominate with increasing volume, as suggested by decreasing height/basal width ratios from the smaller volcanoes towards the larger ones (Fig. 8C and Fig. 10). Massifs, for example, do not develop a single restricted summit, but rather have extensive flat plateaus with multiple vents. Large cones and massifs tend to increase in irregularity as they evolve but their ellipticity does not change significantly (Fig. 8E–F).

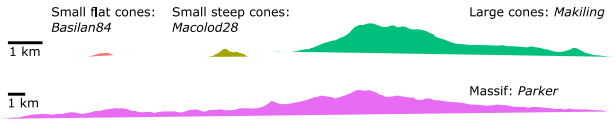

Fig. 10. Cross sections passing through the summit of four representative volcanoes from the four morphometric classes. The Massif profile is presented at half the scale of the other classes.

While there are few andesitic small flat cones, there are many andesitic small steep cones, and the majority of the large cones are andesitic (Fig. 6). The proportion of basalts decreases from small to large cones, and this trend suggests that edifice growth is accompanied by an evolution in the average magma composition, which in turn suggests that the increased load of larger edifices leads to greater degrees of magma differentiation. Numerical modelling shows that the load of an edifice can cause dykes to stall before reaching the surface, allowing magma to evolve by fractional crystallisation or crustal assimilation (Pinel and Jaupart, 2000). In addition, the density threshold below which magmas become buoyant enough to continue ascending is lower for larger loads (Pinel and Jaupart, 2000). This effect has been seen at individual volcanoes, where large edifices have lead to more silicic magmas (e.g., Longpré et al., 2009; Fabbro et al., 2013), and edifice collapses have been followed by more mafic magma reaching the surface (e.g., Hora et al., 2007; Manconi et al., 2009); here we suggest that this process can be seen more generally in the change in composition of Philippine volcanoes as they evolve from small to large cones. Despite this, massifs are dominated by basaltic and andesitic magmas (Fig. 6). A possible explanation for the lack of silicic eruptions from massifs is that silicic magma is more explosive; therefore, any volcano that starts erupting dacite or rhyolite tends to have a destructive explosive eruption, forming a caldera rather than continuing to evolve into a massif. It is also possible that the more distributed eruptions from massifs lead to a more distributed load, allowing less-evolved magma to reach the surface.

During the active lifetime of a volcano, its growth rate is likely to be greater than its erosion or destruction rate; however, during inactivity and quiescence, destructive processes dominated by mass wasting or fluvial erosion gradually take over, reshaping the landscape. Erosion and destruction may become apparent, resulting in a more irregular edifice with uneven slopes, more secondary peaks, reduced height, and lateral transport of material down the flanks. Larger volcanoes tend to be more irregular as they evolve, as a result of either degradation or lateral growth (Fig. 8F). This suggests that although climate and volcano-induced climate could potentially play a role in the edifice development, volcano age correlated with edifice height must also be considered.

Edifice steepness seems to be related to its average magma composition (Fig. 9B), although this may be complicated by geochemical trends or variations at individual volcanoes. As the magma evolves from basalt to andesite, its viscosity and yield strength increases (e.g., Giordano et al., 2008), and this is reflected in steeper slopes; however, as the magma evolves from andesite to dacite and rhyolite, there is a decrease in the steepness of the edifices that could be due to a change in eruptive style. Silicic magmas tend to be more explosive, and explosive eruptions will tend to produce less steep edifices than effusive eruptions. Explosive eruptions are more destructive, potentially lowering the edifice height, and they often generate widespread tephra fall and long runout pyroclastic flow deposits, potentially increasing the basal area. In addition, pyroclastic deposits are more easily eroded. These processes would decrease the height/basal width ratio and the average slope of the edifice and could explain the dominance of andesitic magmas in large cones in the Philippines. The increase in steepness from basaltic small cones to andesitic large cones would concentrate the load of the edifice, which would increase the degree of evolution of the magma, leading to a positive feedback. If the magma composition becomes more silicic than andesite, the decrease in steepness would

lead to more distributed loads, which would reduce the effect of the load on the evolution of the magma.

5.3. Magma propagation and spatial distribution of volcanoes in the volcanic fields

The clustered distribution of edifices in the Basilan, Lanao, Macolod, Makaturing, Maramag, and Zamboanga volcanic fields may be explained by individual batches of magma ascending into the crust, with each batch producing a cluster of volcanoes (Le Corvec et al., 2013). Each batch may have a discrete source, or the source may continuously produce melt that ascends as individual batches. However, it is not clear whether pre-existing crustal structures or crustal heterogeneities influence the development of mid-crustal sills, which can also serve as secondary sources feeding several eruptions at the surface (Kavanagh et al., 2006; Valentine and Krogh, 2006; Macceferri and Bonafede, 2011). If volcanic centre alignments coincide with the long axis of the shape ellipse, as is the case in Basilan, Lanao, and Maramag volcanic fields, and if the dikes ascended vertically, then the shape of the field at the surface would approximately represent the shape of the source in the mantle. However, in the case of the Philippine volcanic fields, there is no geophysical data to support this claim.

Alignments of volcanoes in a volcanic field may be influenced by the stress conditions and the pre-existing structures of the crust and hence can reflect magma propagation and ascent paths (e.g., Nakamura, 1977; Connor, 1987; Connor et al., 1992; Le Corvec et al., 2013; Paguican and Bursik, 2016). The preferred alignments may represent the stress field at the time of intrusion, if the dykes propagated into newly formed cracks oriented perpendicular to the direction of the least principal tectonic stress, σ_3 (Delaney and Pollard, 1981), or they could reflect pre-existing crustal-scale faults (Valentine and Krogh, 2006). Recent work by Gómez-Vasconcelos et al. (2020) has shown that monogenetic volcanoes in the Michoácan-Guanajuato volcanic field in Mexico are aligned along an active fault system. However, vent alignment analysis must be considered with care because of the inherent uncertainty in the method and the selection of points (e.g., Tibaldi, 1995).

Basilan volcanic field, in a compressional tectonic environment (Heidbach et al., 2008), has 93% of its volcanoes preferentially aligned roughly east–west, with some aligned ~60°-70°, parallel to the Sulu trench (Fig. 4, Table 3). We attribute these alignments to magma ascent along pre-existing crustal structures and reactivated faults (Sibson, 1990; Galland et al., 2003).

In the strike-slip environments of the Lanao and Maramag volcanic fields (Fig. 4), one or two preferred alignments along the tectonic features is possible if magma ascends via extension fractures and strike-slip faults, which tend to be vertical. The other preferred orientation may result from rotation of the stress field producing en-echelon structures (Delaney and Pollard, 1981) or the development of flower structures in releasing and restraining bends along strike-slip faults (Sylvester, 1988). This is seen in the growth of Labo and Caayunan volcanoes (Pasquarè and Tibaldi, 2003), where dome shapes and alignments are parallel to the regional transcurrent structure; however, there was a period during its growth where the stress from the magma chamber dominated over the regional stress and domes were aligned radially.

In the Macolod Volcanic Field, the alignments are likely controlled by the associated normal fault system and strike slip faulting from the localized extension described by Galgana et al. (2007). The dominant northeast–southwest alignment of the extensional Macolod Volcanic Field is attributed to the tendency of rift systems to be mechanically segmented along strike (Ebinger et al., 1999). In this case, the kinematic coherence is probably achieved when ascending magma took advantage of cross faults that are at high angle to the rift orientation (Le Gall et al., 2000) that act as transfer zones. These are minor northeast–southwest strike-slip or oblique faults (Förster et al., 1990).

The non-clustered distribution of volcanoes in the Labo and Upi volcanic fields can be explained by a low magma flux or production, similar to the case in the Auckland Volcanic Field (Le Corvec et al., 2013). In this case, the source at depth produces only enough magma for a single eruption.

6. Conclusions

Philippine volcanoes can be classified morphometrically as small flat cones, small steep cones, large cones, and massifs, based on their size, irregularity, number of peaks, and steepness (height/basal width ratio and mean slope), and to a lesser extent on truncation and elongation. Small flat cones are mostly monogenetic, with each volcano having a restricted chemical range. Small steep cones may be monogenetic or polygenetic, and may evolve into large cones, some of which may further grow laterally into massifs. The largest volcanoes, including both large cones and massifs, are in Negros, North and South Mindanao, East Philippines, and West Luzon. Their location coincides with the thickened crust of the Bicol–Negros–Panay, Central Mindanao, and Central Luzon regions, suggesting that the thickness of the crust may have influenced the evolution of magma underneath these volcanoes.

The distribution and alignment of volcanoes in the eight volcanic fields analysed show different controls related to the dominant stress conditions and presence of pre-existing faults. The trend towards more silicic compositions from small to large cones may be attributed to larger edifice loads preventing mafic dykes from reaching the surface, and this in turn may drive magma evolution. More evolved and explosive magmas may cause more silicic volcanoes to be less steep than andesitic ones.

Declaration of Competing Interest

The authors declare that they have no known competing financial interests or personal relationships that could have appeared to influence the work reported in this paper.

Acknowledgements

This work was funded by a 2015 Belgium Science Policy (BELSPO) Postdoctoral Fellowship for non-European researchers. EM Paguican was also funded by the Balik Scientist Fellowship from the Philippine Department of Science and Technology to continue writing this manuscript. GF received funding support from the Earth Observatory of Singapore via its funding from the National Research Foundation Singapore and the Singapore Ministry of Education under the Research Centres of Excellence initiative. Many thanks to the editor, Dr. Jose Luis Macias, and to the reviewers Dr. Alessandro Tibaldi and an anonymous reviewer for their helpful comments.

Appendix A. Supplementary data

Supplementary data to this article can be found online at https://doi.org/10.1016/j.jvolgeores.2021.107251.

References

Andal, E.S., Yumul, G.P., Listanco, E.L., Tamayo, R.A., Dimalanta, C.B., Ishii, T., 2005. Characterization of the Pleistocene volcanic chain of the bicol arc, Philippines: implications for geohazard assessment. Terr. Atmos. Ocean. Sci. 16, 865–883. https://doi.org/10.3319/TAO.2005.16.4.865(GIG).

Armada, L.T., Hsu, S.K., Ku, C.Y., Doo, W.B., Wu, W.N., Dimalanta, C., Yumul, G.P., 2012. Possible northward extension of the Philippine Fault Zone offshore Luzon Island (Philippines). Mar. Geophys. Res. 33, 369–377. https://doi.org/10.1007/s11001-013-9169-5.

Aurelio, M., 2000. Tectonics of the Philippines revisited. J. Geol. Soc. Philip. 55, 119–183.

Aurelio, M., Pena, R., 2002. Geology and Mineral Resources of the Philippines- Volume 1: Geology. Technical Report. Department of Environment and Natural Resources-Mines and Geosciences Bureau, Quezon City.

Baloga, S.M., Glaze, L.S., Bruno, B.C., 2007. Nearest-neighbor analysis of small features on Mars: applications to tumuli and rootless cones. J. Geophys. Res. 112. https://doi.org/10.1029/2005JE002652 E03002.

Barrier, E., Huchon, P., Aurelio, M., 1991. Philippine Fault: a key for Philippine kinematics. Geology 19, 32–35. https://doi.org/10.1130/0091-7613(1991)019<0032:PFAKFP>2.3.CO;2.

Beggan, C.D., Hamilton, C.W., 2010. New image processing software for analyzing object size-frequency distributions, geometry, orientation, and spatial distribution. Comput. Geosci. 36, 539–549. https://doi.org/10.1016/j.cageo.2009.09.003.

Bernard, B., Takarada, S., Andrade, S.D., Dufresne, A., 2020. Terminology and strategy to describe volcanic landslides and debris avalanches. In: Roverato, M., Dufresne, A., Procter, J.N. (Eds.), Volcanic Debris Avalanches: From Collapse to Hazard. Springer Book Series Advances in Volcanology. Springer Book Series Advances in Volcanology https://doi.org/10.1007/978-3-030-57411-6_3.

Besana, G., Negishi, H., Ando, M., 1997. The three-dimensional attenuation structures beneath the Philippine archipelago based on seismic intensity data inversion. Earth Planet. Sci. Lett. 151, 1–11. https://doi.org/10.1016/S0012-821X(97)00112-X.

Bleacher, J.E., Glaze, L.S., Greeley, R., Hauber, E., Baloga, S.M., Sakimoto, S.E.H., Williams, D. A., Glotch, T.D., 2009. Spatial and alignment analyses for a field of small volcanic vents south of Pavonis Mons and implications for the Tharsis province, Mars. J. Volcanol. Geotherm. Res. 185, 96–102. https://doi.org/10.1016/j.jvolgeores.2009.04.008.

Calibo, M., Honrado, M., Paguican, E.M., Listanco, E., 2009. Monogenetic fields in the Macolod Corridor. NIGS Research Symposium 2010: Dangerous Grounds: A Geological Perspective on Philippine Disasters, Quezon City.

Carr, M.J., 1984. Symmetrical and segmented variation of physical and geochemical characteristics of the central american volcanic front. J. Volcanol. Geotherm. Res. 20, 231–252. https://doi.org/10.1016/0377-0273(84)90041-6.

Castillo, P.R., Newhall, C.G., 2004. Geochemical constraints on possible subduction components in lavas of Mayon and Taal Volcanoes, Southern Luzon, Philippines. J. Petrol. 45, 1089–1108. https://doi.org/10.1093/petrology/egh005.

Castillo, P.R., Janney, P.E., Solidum, R.U., 1999. Petrology and geochemistry of Camiguin Island, southern Philippines: insights to the source of adakites and other lavas in a complex arc setting. Contrib. Mineral. Petrol. 134, 33–51. https://doi.org/10.1007/s004100050467.

Clark, P.J., Evans, F.C., 1954. Distance to nearest neighbor as a measure of spatial relationships in populations. Ecol. Soc. Am. 35, 445–453.

Condit, C.D., Connor, C.B., 1996. Recurrence rates of volcanism in basaltic volcanic fields: an example from the Springerville volcanic field, Arizona. Geol. Soc. Am. Bull. 108, 1225–1241.

Connor, C.B., 1987. Structure of the Michoacán–Guanajuato Volcanic Field, Mexico. J. Volcanol. Geotherm. Res. 33, 191–200. https://doi.org/10.1016/0377-0273(87)90061-8.

Connor, C.B., Condit, C.D., Crumpler, L.S., Aubele, J.C., 1992. Evidence of regional structural controls on vent distribution: Springerville Volcanic Field, Arizona. J. Geophys. Res. 97, 12,349–12,359. https://doi.org/10.1029/92JB00929.

Corazzato, C., Tibaldi, A., 2006. Fracture control on type, morphology and distribution of parasitic volcanic cones: an example from Mt. Etna, Italy. J. Volcanol. Geotherm. Res. 158, 177–194. https://doi.org/10.1016/j.jvolgeores.2006.04.018.

Corpuz, E.S., 1992. Petrology and Geochemistry of the Central Mindanao Volcanic Arc, Southern Philippines. Ph.d. thesis. University of Canterbury URL: http://hdl.handle.net/10092/5789.

Defant, M.J., Maury, R., Joron, J.L., Feigenson, M.D., Leterrier, J., Bellon, H., Jacques, D., Richard, M., 1990. The geochemistry and tectonic setting of the northern section of the Luzon arc (The Philippines and Taiwan). Tectonophysics 183, 187–205. https://doi.org/10.1016/0040-1951(90)90416-6.

Defant, M.J., Maury, R.C., Ripley, E.M., Feigenson, M.D., Jacques, D., 1991. An example of Island-arc petrogenesis: geochemistry and petrology of the Southern Luzon arc, Philippines. J. Petrol. 32, 455–500. https://doi.org/10.1093/petrology/32.3.455.

Delaney, P.T., Pollard, D., 1981. Deformation of Host Rocks and Flow of Magma during Growth of Minette Dikes and Breccia-bearing Intrusions near Ship Rock, New Mexico Geological survey professional paper, 69.

Delfin, F.G., Panem, C.C., Defant, M.J., 1993. Eruptive history and petrochemistry of the Bulusan volcanic complex: implications for the hydrothermal system and volcanic hazards of Mt. Bulusan, Philippines. Geothermics 22, 417–434. https://doi.org/10.1016/0375-6505(93)90029-M.

Ebinger, C.J., Jackson, J.a., Foster, A.N., Hayward, N.J., 1999. Extensional basin geometry and the elastic lithosphere. Philos. Trans. R. Soc. A Math. Phys. Eng. Sci. 357, 741–765. https://doi.org/10.1098/rsta.1999.0351.

Fabbro, G.N., Druitt, T.H., Scaillet, S., 2013. Evolution of the crustal magma plumbing system during the build-up to the 22-ka caldera-forming eruption of Santorini (Greece). Bull. Volcanol. 75, 1–22. https://doi.org/10.1007/s00445-013-0767-5.

Farner, M.J., Lee, C.T.A., 2017. Effects of crustal thickness on magmatic differentiation in subduction zone volcanism: a global study. Earth Planet. Sci. Lett. 470, 96–107. https://doi.org/10.1016/j.epsl.2017.04.025.

Förster, H., Oles, D., Knittel, U., Defant, M.J., Torres, R.C., 1990. The Macolod Corridor: a rift crossing the Philippine island arc. Tectonophysics 183, 265–271. https://doi.org/10.1016/0040-1951(90)90420-D.

Galgana, G., Hamburger, M., McCaffrey, R., Corpuz, E.S., Chen, Q., 2007. Analysis of crustal deformation in Luzon, Philippines using geodetic observations and earthquake focal mechanisms. Tectonophysics 432, 63–87. https://doi.org/10.1016/j.tecto.2006.12.001.

Galland, O., de Bremond d'Ars, J., Cobbold, P.R., Hallot, E., 2003. Physical models of magmatic intrusion during thrusting. Terra Nova 15, 405–409. https://doi.org/10.1046/j.1365-3121.2003.00512.x.

Gervasio, F., 1967. Age and nature of orogenesis of the Philippines. Tectonophysics 4, 379–402. https://doi.org/10.1016/0040-1951(67)90006-6.

Giordano, D., Russell, J.K., Dingwell, D.B., 2008. Viscosity of magmatic liquids : a model. Earth Planet. Sci. Lett. 271, 123–134. https://doi.org/10.1016/j.epsl.2008.03.038.

Gómez-Vasconcelos, M.G., Macías, J.L., Avellán, D.R., Sosa-Ceballos, G., Garduño-Monroy, V.H., Cisneros-Máximo, G., Layer, P.W., Benowitz, J., López-Loera, H., López, F.M., Perton, M., 2020. The control of preexisting faults on the distribution, morphology, and volume of monogenetic volcanism in the Michoacán-Guanajuato Volcanic Field. GSA Bull. 132, 2455–2474. https://doi.org/10.1130/b35397.1.

Grosse, P., van Wyk de Vries, B., Petrinovic, I.A., Euillades, P.A., Alvarado, G.E., 2009. Morphometry and evolution of arc volcanoes. Geology 37, 651–654. https://doi.org/10.1130/G25734A.1.

Grosse, P., van Wyk de Vries, B., Euillades, P.A., Kervyn, M., Petrinovic, I.A., 2012. Systematic morphometric characterization of volcanic edifices using digital elevation models. Geomorphology 136, 114–131. https://doi.org/10.1016/j.geomorph.2011.06.001.

Grosse, P., Euillades, P.A., Euillades, L.D., van Wyk de Vries, B., 2014. A global database of composite volcano morphometry. Bull. Volcanol. 76, 784. https://doi.org/10.1007/s00445-013-0784-4.

Hamilton, C.W., Fagents, S.A., Thordarson, T., 2010. Explosive lava–water interactions II: self-organization processes among volcanic rootless eruption sites in the 1783–1784 Laki lava flow, Iceland. Bull. Volcanol. 72, 469–485. https://doi.org/10.1007/s00445-009-0331-5.

Heidbach, O., Tingay, M., Barth, A., Reinecker, J., Kurfeß, D., Müller, B., 2008. The World Stress Map Database Release 2008. https://doi.org/10.1594/GFZ.WSM.Rel2008.

Hora, J.M., Singer, B.S., Wörner, G., 2007. Volcano evolution and eruptive flux on the thick crust of the Andean Central Volcanic Zone: $^{40}Ar/^{39}Ar$ constraints from Volcán Parinacota, Chile. Bull. Geol. Soc. Am. 119, 343–362. https://doi.org/10.1130/B25954.1.

Hsu, Y.J., Yu, S.B., Loveless, J.P., Bacolcol, T., Solidum Jr., R., Pelicano, A., Woessner, J., 2016. Journal of Geophysical Research : Solid Earth. J. Geophys. Res. Solid Earth 121, 7639–7665. https://doi.org/10.1002/2016JB013082.Received.

Jolliffe, I., 2002. Principal components analysis. Second ed. Springer-Verlag, New York https://doi.org/10.1007/b98835.

Karátson, D., Thouret, J.C., Moriya, I., Lomoschitz, A., 1999. Erosion calderas: Origins, processes, structural and climatic control. Bull. Volcanol. 61, 174–193. https://doi.org/10.1007/s004450050270.

Karlstrom, L., Dufek, J., Manga, M., 2009. Organization of volcanic plumbing through magmatic lensing by magma chambers and volcanic loads. J. Geophys. Res. Solid Earth 114, 1–16. https://doi.org/10.1029/2009JB006339.

Kavanagh, J.L., Menand, T., Sparks, R.S.J., 2006. An experimental investigation of sill formation and propagation in layered elastic media. Earth Planet. Sci. Lett. 245, 799–813. https://doi.org/10.1016/j.epsl.2006.03.025.

Knittel, U., Oles, D., 1994. Basaltic volcanism associated with extensional tectonics in the Taiwan-Luzon island arc: evidence for non-depleted sources and subduction zone enrichment. Geol. Soc. Spec. Publ. 81, 77–93. https://doi.org/10.1144/GSL.SP.1994.081.01.05.

Köhn, H., Hubert, L.J., 2015. Hierarchical Cluster Analysis, in: Wiley StatsRef: Statistics Reference Online. American Cancer Society, pp. 1–13 https://doi.org/10.1002/9781118445112.stat02449.pub2.

Lagmay, A.M.F.A., Valdivia, W., 2006. Regional stress influence on the opening direction of crater amphitheaters in Southeast Asian volcanoes. J. Volcanol. Geotherm. Res. 158, 139–150. https://doi.org/10.1016/j.jvolgeores.2006.04.020.

Lagmay, A.M.F.A., van Wyk de Vries, B., Kerle, N., Pyle, D.M., 2000. Volcano instability induced by strike-slip faulting. Bull. Volcanol. 62, 331–346. https://doi.org/10.1007/s004450000103.

Le Corvec, N., Spörli, K.B., Rowland, J., Lindsay, J., 2013. Spatial distribution and alignments of volcanic centers: Clues to the formation of monogenetic volcanic fields. Earth Sci. Rev. 124, 96–114. https://doi.org/10.1016/j.earscirev.2013.05.005.

Le Gall, B., Tiercelin, J.J., Richert, J.P., Gente, P., Sturchio, N.C., Stead, D., Le Turdu, C., 2000. A morphotectonic study of an extensional fault zone in a magma-rich rift: the Baringo Trachyte Fault System, Central Kenya Rift. Tectonophysics 320, 87–106. https://doi.org/10.1016/S0040-1951(00)00069-X.

Le Maitre, R.W., Streckeisen, A., Zanettin, B., Le Bas, M.J., Bonin, B., Bateman, P., Bellieni, G., Dudek, A., Schmid, R., Sørensen, H., Woolley, A.R., 2005. Igneous Rocks: A Classification and Glossary of Terms: Recommendation of the International Union of Geological Sciences, Subcommission on the Systematics of Igneous Rocks. 2nd ed. Cambridge University Press, Cambridge.

Longpré, M.A., Troll, V.R., Walter, T.R., Hansteen, T.H., 2009. Volcanic and geochemical evolution of the Teno massif, Tenerife, Canary Islands: some repercussions of giant landslides on ocean island magmatism. Geochem. Geophys. Geosyst. 10. https://doi.org/10.1029/2009GC002892.

Macceferri, F., Bonafede, M., 2011. A quantitative study of the mechanisms governing dike propagation, dike arrest and sill formation. J. Volcanol. Geotherm. Res. 1-2, 39–50. https://doi.org/10.1016/j.jvolgeores.2011.09.001.

Manconi, A., Longpré, M.A., Walter, T.R., Troll, V.R., Hansteen, T.H., 2009. The effects of flank collapses on volcano plumbing systems. Geology 37, 1099–1102. https://doi.org/10.1130/G30104A.1.

McDermott, F., Delfin, F.G., Defant, M.J., Turner, S., Maury, R., 2005. The petrogenesis of volcanics from Mt. Bulusan and Mt. Mayon in the Bicol arc, the Philippines. Contrib. Mineral. Petrol. 150, 652–670. https://doi.org/10.1007/s00410-005-0042-7.

McGuire, W.J., 1996. Volcano instability: A review of contemporary themes. Volcano Instability on the Earth and other Planets. 110, pp. 1–23. https://doi.org/10.1144/gsl.sp.1996.110.01.01.

Miklius, A., Flower, M.F., Huijsmans, J.P., Mukasa, S.B., Castillo, P.R., 1991. Geochemistry of lavas from Taal Volcano, southwestern Luzon, Philippines: evidence for multiple magma supply systems and mantle source heterogeneity. J. Petrol. 32, 593–627. https://doi.org/10.1093/petrology/32.3.593.

Nakamura, K., 1977. Volcanoes as possible indicators of tectonic stress orientation-principle and proposal. J. Volcanol. Geotherm. Res. 2, 1–16.
Paguican, E.M., Bursik, M., 2016. Tectonic geomorphology and volcano-tectonic interaction in the eastern boundary of the Southern Cascades (Hat Creek Graben Region), California, USA. Front. Earth Sci. 4. https://doi.org/10.3389/feart.2016.00076.
Paguican, E.M., van Wyk de Vries, B., Lagmay, A.M.F.A., 2012. Volcano-tectonic controls and emplacement kinematics of the Iriga debris avalanches (Philippines). Bull. Volcanol. 74, 2067–2081. https://doi.org/10.1007/s00445-012-0652-7.
Pansino, S., Taisne, B., 2019. How magmatic storage regions attract and repel propagating dikes. J. Geophys. Res. Solid Earth 124, 274–290. https://doi.org/10.1029/2018JB016311.
Parcutela, N.E., Dimalanta, C.B., Armada, L.T., Yumul, G.P., 2020. PHILCRUST3.0: new constraints in crustal growth rate computations for the Philippine arc. J. Asian Earth Sci. https://doi.org/10.1016/j.jaesx.2020.100032 X, 100032.
Pasquarè, F.A., Tibaldi, A., 2003. Do transcurrent faults guide volcano growth? The case of NW Bicol Volcanic Arc, Luzon, Philippines. Terra Nova 15, 204–212. https://doi.org/10.1046/j.1365-3121.2003.00484.x.
Philippine Institute of Volcanology and Seismology, 2008. Classification of Volcanoes. URL. http://www.phivolcs.dost.gov.ph/.
Pinel, V., Jaupart, C., 2000. The effect of edifice load on magma ascent beneath a volcano. Philos. Trans. R. Soc. A Math. Phys. Eng. Sci. 358, 1515–1532. https://doi.org/10.1098/rsta.2000.0601.
Pubellier, M., Quebral, R., Rangin, C., Deffontaines, B., Muller, C., Butterlin, J., Manzano, J., 1991. The Mindanao Collision Zone: a soft collision event within a continuous Neogene strike-slip setting. J. SE Asian Earth Sci. 6, 239–248. https://doi.org/10.1016/0743-9547(91)90070-E.
Ramalho, R.S., Quartau, R., Trenhaile, A.S., Mitchell, N.C., Woodroffe, C.D., Ávila, S.P., 2013. Coastal evolution on volcanic oceanic islands: a complex interplay between volcanism, erosion, sedimentation, sea-level change and biogenic production. Earth Sci. Rev. 127, 140–170. https://doi.org/10.1016/j.earscirev.2013.10.007.
Sajona, F.G., Maury, R.C., Bellon, H., Cotten, J., Defant, M.J., Pubellier, M., 1993. Initiation of subduction and the generation of slab melts in western and eastern Mindanao, Philippines. Geology 21, 1007–1010. https://doi.org/10.1130/0091-7613(1993)021<1007:IOSATG>2.3.CO;2.
Sajona, F.G., Bellon, H., Maury, R.C., Pubellier, M., Cotten, J., Rangin, C., 1994. Magmatic response to abrupt changes in geodynamic settings: Pliocene-Quaternary calc-alkaline and Nb-enriched lavas from Mindanao (Philippines). Tectonophysics 237, 47–72. https://doi.org/10.1016/0040-1951(94)90158-9.
Sajona, F.G., Maury, R.C., Bellon, H., Cotten, J., Defant, M.J., 1996. High field strength element enrichment of Pliocene-Pleistocene Island arc basalts, Zamboanga Peninsula, western Mindanao (Philippines). J. Petrol. 37, 693–726. https://doi.org/10.1093/petrology/37.3.693.
Sajona, F.G., Bellon, H., Maury, R.C., Pubellier, M., Quebral, R.D., Cotten, J., Bayon, F.E., Pagado, E., Pamatian, P., 1997. Tertiary and quaternary magmatism in Mindanao and Leyte (Philippines): geochronology, geochemistry and tectonic setting. J. Asian Earth Sci. 15, 121–153 URL: http://linkinghub.elsevier.com/retrieve/pii/S0743954797000020. https://doi.org/10.1016/S0743-9547(97)00002-0.
Sajona, F.G., Maury, R.C., Prouteau, G., Cotten, J., Schiano, P., Bellon, H., Fontaine, L., 2000. Slab melt as metasomatic agent in island arc magma mantle sources, Negros and Batan (Philippines). Island Arc 9, 472–486. https://doi.org/10.1046/j.1440-1738.2000.00295.x.
Sibson, R.H., 1990. Conditions for fault-valve behaviour. In: Knipe, R.J., Rutter, E.H. (Eds.), Deformation Mechanism. Rheology and Tectonics. Geological Society Special Publication vol. 54, pp. 15–28.
Sylvester, A.G., 1988. Strike-slip faults. Geol. Soc. Am. Bull. 100, 1666–1703. https://doi.org/10.1130/0016-7606(1988)100<1666.
Thouret, J.C., Oehler, J.F., Gupta, A., Solikhin, A., Procter, J.N., 2014. Erosion and aggradation on persistently active volcanoes – a case study from Semeru Volcano, Indonesia. Bull. Volcanol. 76. https://doi.org/10.1007/s00445-014-0857-z.
Tibaldi, A., 1995. Morphology of pyroclastic cones and tectonics. J. Geophys. Res. 100, 24,521–24,535. https://doi.org/10.1029/95JB02250.
Tibaldi, A., Corazzato, C., Kozhurin, A., Lagmay, A.M.F.A., Pasquarè, F.A., Ponomareva, V.V., Rust, D., Tormey, D., Vezzoli, L., 2008. Influence of substrate tectonic heritage on the evolution of composite volcanoes: predicting sites of flank eruption, lateral collapse, and erosion. Glob. Planet. Chang. 61, 151–174. https://doi.org/10.1016/j.gloplacha.2007.08.014.
Valentine, G.A., Krogh, K., 2006. Emplacement of shallow dikes and sills beneath a small basaltic volcanic center – the role of pre-existing structure (Paiute Ridge, southern Nevada, USA). Earth Planet. Sci. Lett. 246, 217–230. https://doi.org/10.1016/j.epsl.2006.04.031.
Vogel, T.A., Flood, T.P., Patino, L.C., Wilmot, M.S., Maximo, R.P.R., Arpa, C.B., Arcilla, C.A., Stimac, J.A., 2006. Geochemistry of silicic magmas in the Macolod Corridor, SW Luzon, Philippines: evidence of distinct, mantle-derived, crustal sources for silicic magmas. Contrib. Mineral. Petrol. 151, 267–281. https://doi.org/10.1007/s00410-005-0050-7.
Wadge, G., Cross, A., 1988. Quantitative methods for detecting aligned points: an application to the volcanic vents of the Michoacan-Guanajuato volcanic field, Mexico. Geology 16, 815–818. https://doi.org/10.1130/0091-7613(1988)016<0815:QMFDAP>2.3.CO;2.
Yumul, G.P., Dimalanta, C., Bellon, H., Faustino, D.V., De Jesus, J.V., Tamayo, R.A., Jumawan, F.T., 2000a. Adakitic lavas in the Central Luzon back-arc region, Philippines: lower crust partial melting products? Island Arc 9, 499–512. https://doi.org/10.1046/j.1440-1738.2000.00297.x.
Yumul, G.P., Dimalanta, C.B., Tamayo Jr., R.A., Barretto, J.A.L., 2000b. Thematic Article Contrasting Morphological Trends of Islands in Central Philippines. The Island Arc. 9, pp. 627–637. https://doi.org/10.1046/j.1440-1738.2000.00307.x.
Yumul, G.P., Dimalanta, C.B., Tamayo, R.A., 2005. Indenter-tectonics in the Philippines: example from the Palawan Microcontinental Block – Philippine Mobile Belt Collision. Resour. Geol. 55, 189–198. https://doi.org/10.1111/j.1751-3928.2005.tb00240.x.
Yumul, G.P., Dimalanta, C.B., Maglambayarw, V.B., Marquez, E.J., 2008. Tectonic setting of a composite terrane: a review of the Philippine island arc system. Geosci. J. 12, 7–17. https://doi.org/10.1007/s12303-008-0002-0.